Molecular Microbiology (2018) 110(5), 811–830 ■
doi:10.1111/mmi.14126
First published online 21 October 2018

AbmR (Rv1265) is a novel transcription factor of *Mycobacterium tuberculosis* that regulates host cell association and expression of the non-coding small RNA Mcr11

Roxie C. Girardin,[1] Guangchun Bai,[2] Jie He,[3] Haixin Sui[1,3] and Kathleen A. McDonough[1,3]*

[1]*Department of Biomedical Sciences, School of Public Health, University at Albany, PO Box 22002, Albany, NY 12201-2002, USA.*
[2]*Department of Immunology and Microbial Disease, Albany Medical College, Albany, NY USA.*
[3]*Wadsworth Center, New York State Department of Health, Albany, NY USA.*

Summary

Gene regulatory networks used by *Mycobacterium tuberculosis* (Mtb) during infection include many genes of unknown function, confounding efforts to determine their roles in Mtb biology. Rv1265 encodes a conserved hypothetical protein that is expressed during infection and in response to elevated levels of cyclic AMP. Here, we report that Rv1265 is a novel auto-inhibitory ATP-binding transcription factor that upregulates expression of the small non-coding RNA Mcr11, and propose that Rv1265 be named ATP-binding *mcr11* regulator (AbmR). AbmR directly and specifically bound DNA, as determined by electrophoretic mobility shift assays, and this DNA-binding activity was enhanced by AbmR's interaction with ATP. Genetic knockout of *abmR* in Mtb increased *abmR* promoter activity and eliminated growth phase-dependent increases in *mcr11* expression during hypoxia. Mutagenesis identified arginine residues in the carboxy terminus that are critical for AbmR's DNA-binding activity and gene regulatory function. Limited similarity to other DNA- or ATP-binding domains suggests that AbmR belongs to a novel class of DNA- and ATP-binding proteins. AbmR was also found to form large organized structures in solution and facilitate the serum-dependent association of Mtb with human lung epithelial cells. These results indicate a potentially complex role for AbmR in Mtb biology.

Accepted 9 September, 2018. *For correspondence. E-mail kathleen.mcdonough@health.ny.gov; Tel. (518) 486-4253; Fax (518) 402-4773.

Introduction

Tuberculosis, caused by the slow-growing bacterium *Mycobacterium tuberculosis* (Mtb), remains a leading cause of death worldwide. The rising prevalence of multiple drug-resistant and extremely drug-resistant Mtb is also a major concern (WHO, 2016). The World Health Organization (WHO) has reported that new diagnostics, drugs and vaccines are needed to attain the goals set in the End TB Strategy, and this requires better understanding of the basic biology and pathogenesis of Mtb (WHO, 2015).

Publication of the curated Mtb genomic sequence (Cole *et al.*, 1998) considerably advanced the characterization of central metabolic processes and virulence determinants in Mtb (Lamichhane *et al.*, 2003; Sassetti and Rubin, 2003; Sassetti *et al.*, 2003; WHO, 2016). Still, nearly one-third of protein-coding genes of Mtb are classified as genes of unknown function or conserved hypothetical proteins (CHPs) (Camus *et al.*, 2002). Bioinformatic approaches have identified probable functional categories for many CHPs of Mtb; however, experimental validation of predicted protein function for such genes is generally lacking (Doerks *et al.*, 2012; Mazandu and Mulder, 2012). The absence of functional information for CHPs is particularly problematic for Mtb, as many genes of unknown function contribute to Mtb virulence and pathogenesis (Sassetti and Rubin, 2003; Goodacre *et al.*, 2014).

The first step of TB pathogenesis is the successful invasion of macrophages and/or host lung epithelial cells by Mtb, which can occur through multiple pathways (Bermudez and Sangari, 2001). The presence of serum strongly influences these interactions (Bermudez and Sangari, 2001). Several bacterial factors involved in Mtb's adherence and invasion of host cells have been described, but gene deletion studies suggest additional undiscovered bacterial components may be involved in

this initial step of pathogenesis (Menozzi *et al*., 1996; Pethe *et al*., 2001; Mueller-Ortiz *et al*., 2002; Reddy and Hayworth, 2002; Vidal Pessolani *et al*., 2003; Menozzi *et al*., 2006; Ramsugit *et al*., 2016).

Successful invasion of host lung tissue by Mtb results in the formation of incipient lesions that mature into confined, organized structures called granulomas (Pai *et al*., 2016). Granulomas, the hallmark of Mtb infection, are hypoxic in guinea pigs, non-human primates and humans (Tsai *et al*., 2006; Via *et al*., 2008). Bacterial adaptation to the hypoxic environment of a mature granuloma is critical for the persistence of Mtb in non-human primates (Majumdar *et al*., 2012; Mehra *et al*., 2015). Mtb's adaptation to host conditions during infection requires gene regulation, so elucidating the gene regulatory networks used by Mtb to sense and respond to host-associated environments may facilitate the design of targeted therapeutics (Shi *et al*., 2005; Garton *et al*., 2008; Galagan *et al*., 2013; Gautam *et al*., 2015; Banerjee *et al*., 2016; Du *et al*., 2016; Flentie *et al*., 2016; Iona *et al*., 2016; Sharp *et al*., 2016).

The universal second messenger molecule 3′, 5′ cyclic adenosine monophosphate (cAMP) is a global regulator of gene expression within Mtb, while secreted cAMP modulates Mtb's interactions with host macrophages (Lowrie *et al*., 1979; Agarwal *et al*., 2009; Bai *et al*., 2009; Nambi *et al*., 2013; Kahramanoglou *et al*., 2014; Knapp *et al*., 2015; Ranganathan *et al*., 2016; Johnson *et al*., 2017). cAMP levels affect the gene regulatory activities of two virulence-associated CRP/FNR family transcription factors in Mtb, Cmr and CRP_{Mt} (Bai *et al*., 2005; Rickman *et al*., 2005; Kahramanoglou *et al*., 2014; Ranganathan *et al*., 2016). We previously identified gene of unknown function Rv1265 as a direct regulatory target of Cmr (Gazdik and McDonough, 2005; Ranganathan *et al*., 2016). Rv1265 encodes a CHP whose expression is induced early during macrophage infection and in response to starvation or elevated levels of cAMP during hypoxia (Betts *et al*., 2002; Hobson *et al*., 2002; Gazdik *et al*., 2009). Additionally, it has been proposed that Rv1265 has a role in bacterial survival during macrophage infection (Luo *et al*., 2016).

Rv1265 is encoded on the chromosome adjacent to the divergent sRNA gene (*mcr11*) (Fig. 1A), downstream of an acid-responsive adenylyl cyclase gene (*Rv1264*), and upstream of the gene encoding mammalian-like serine-threonine protein kinase (STPK) PknH (*Rv1266c*) (Tews *et al*., 2005; Zheng *et al*., 2007; DiChiara *et al*., 2010; Arnvig *et al*., 2011; Pelly *et al*., 2012). Mcr11 expression is regulated in response to cAMP levels, by advanced growth phase, and in the lungs of infected mice (DiChiara *et al*., 2010; Arnvig *et al*., 2011; Pelly *et al*., 2012). Overexpression of Mcr11 has been linked with growth arrest in Mtb (Arnvig and Young, 2009; Ignatov *et al*., 2015), but the gene regulatory factors that control Mcr11 expression have not been identified. Genomic co-localization can be indicative of functional linkages among the gene products in bacteria, so we were intrigued by the immediate proximity of *Rv1265* to three genes associated with environmental signaling and/or gene regulation.

We demonstrate that Rv1265 is a novel transcription factor that binds both ATP and DNA and directly regulates the expression of itself and the sRNA Mcr11. Our analysis suggests that Rv1265 belongs to a novel class of DNA- and ATP-binding proteins, and we propose ATP-binding *mcr11* regulator (*abmR*) as a name for *Rv1265*. AbmR is required for serum-dependent invasion of Mtb in A549 human lung epithelial cells, but does not affect Mtb survival in macrophages. This study highlights the critical value of secondary structure-based bioinformatics algorithms as tools for experimental discovery and characterizing genes of unknown function.

Results

Prediction and confirmation of abmR *function*

Previous studies showed that *abmR* (*Rv1265*) is expressed early during macrophage infection, during nutrient starvation and in response to hypoxia with elevated cAMP levels (Betts *et al*., 2002; Hobson *et al*., 2002; Gazdik and McDonough, 2005; Gazdik *et al*., 2009). However, multiple BLAST analyses of *abmR* nucleotide and predicted amino acid sequences provided no information regarding the potential function of AbmR. In contrast, a bioinformatic search for secondary structure-based domains using Phyre^2 (Kelley and Sternberg, 2009) yielded three hits in the C-terminus of AbmR for nucleic acid-binding domains with 17–35% sequence coverage and 36.3–50.4% confidence (Figs 1A and S1). Despite the relatively low confidence score, results of this Phyre^2 search were similar to those obtained when the annotated amino acid sequence of AbmR was modeled in a genome-wide study predicting mycobacterial protein functions (Mao *et al*., 2013). Therefore, we experimentally addressed the possibility that AbmR has nucleic acid-binding activity.

Full-length recombinant His-AbmR was purified to greater than 95% purity (Fig. S1B), and electrophoretic mobility shift assays (EMSAs) were used to test AbmR's ability to bind DNA or RNA substrates. Purified AbmR directly and specifically bound a double-stranded DNA probe covering the intergenic region upstream of AbmR, between the *mcr11* and the *abmR* genes. AbmR binding to this DNA probe produced a pattern of multiple shifted bands, which were competed away by excess specific unlabeled competitor, but not by a non-specific DNA fragment (Fig. 1B). In contrast, AbmR did not bind an RNA probe containing either the sRNA Mcr11, or the complete intergenic region between *Rv1264* and *abmR* (Fig. S1C).

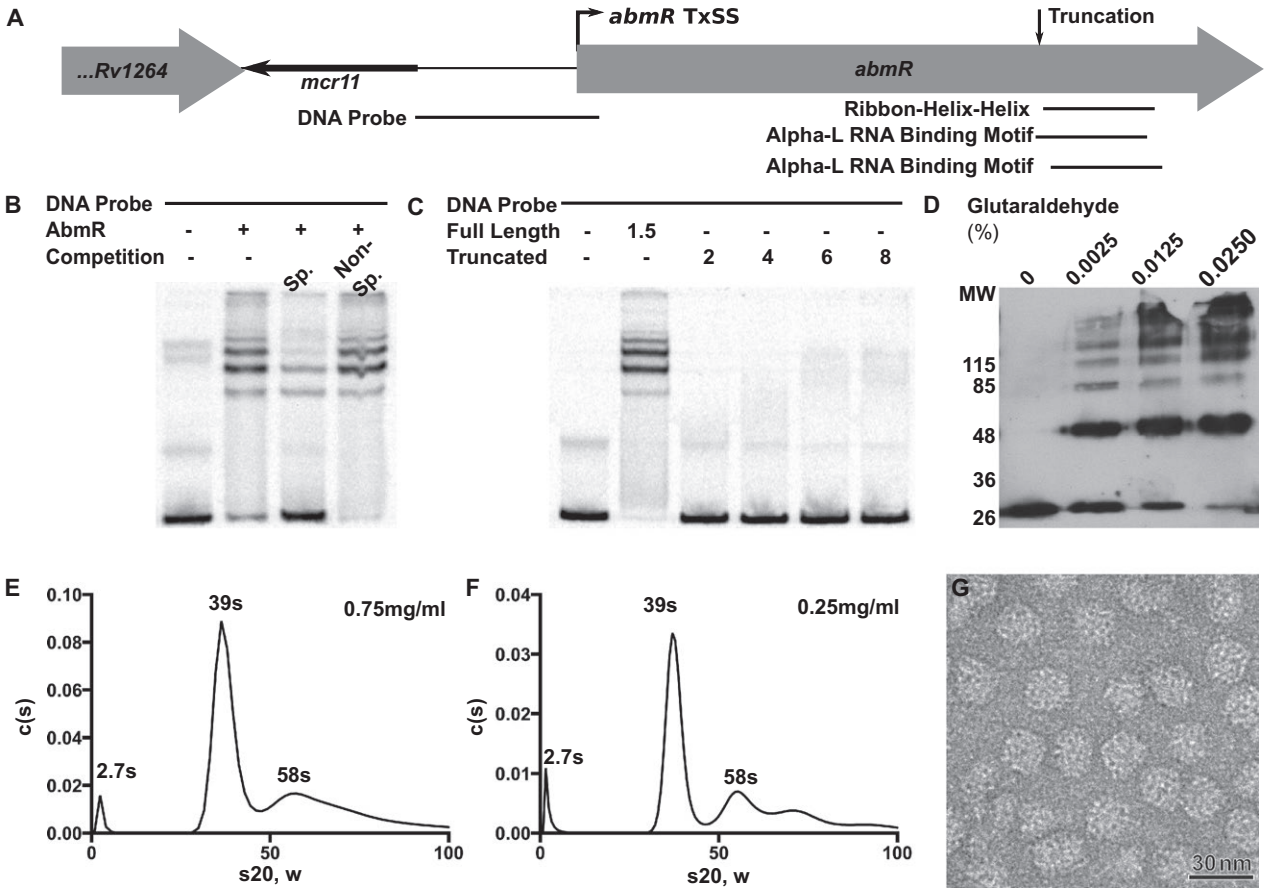

Fig. 1. AbmR is a DNA-binding protein.
A. A cartoon demonstrates the orientation of the corrected AbmR ORF in Mtb. The locations of Phyre[2] hits are denoted with black bars and an arrow indicates the point of truncation of mutant protein used in (C). A red bar illustrates the region of DNA used to probe for DNA binding.
B. The DNA-binding activity of 1.5 μM AbmR was assayed by EMSA in the presence of 5 mM ATP; competitors for binding included 250-fold excess unlabeled non-specific (Non-sp.) competitor DNA or 250-fold excess unlabeled specific (Sp.) competitor DNA.
C. The DNA-binding activity of recombinant AbmR truncated at the putative nucleic acid binding domain was assayed by EMSA in the presence of 5 mM ATP. The μM concentration of protein added is indicated.
D. Western blot analysis of 500 nM purified recombinant AbmR protein in the presence of indicated concentrations of glutaraldehyde.
E. Analytical ultracentrifugation analysis of 0.75 mg ml^{-1} wild-type AbmR protein in 20 mM HEPES, 150 mM NaCl, pH 8.0.
F. As in (E), but with 0.25 mg ml^{-1} wild-type AbmR protein.
G. Transmission electron micrograph of negatively stained recombinant AbmR at 100,000x magnification with wild-type protein. Black scale bar is 30 nm. Results representative of three independent experiments.

Thus, we conclude that AbmR either does not bind RNA or it binds unknown RNA targets. These results demonstrate the specificity of AbmR binding to the DNA region upstream of the *abmR* open reading frame (ORF).

Phyre[2] predicted that the nucleic acid-binding region of AbmR was located in its carboxy (C-) terminus (Fig. 1A). A truncated version of AbmR lacking this predicted nucleic acid-binding region (amino acids 130–189) failed to bind a DNA probe containing the *mcr11-abmR* intergenic region, even at a concentration of 8 μM (Fig. 1C). Together, these data establish that AbmR is a DNA-binding protein, and suggest that the C-terminus is required for this binding activity.

Many bacterial transcription factors (TFs) oligomerize to modulate their regulatory activity, so we investigated the oligomerization status of AbmR protein. Full-length AbmR migrated at a position consistent with a protein of 26 kilodaltons (kDa) in SDS-PAGE, which is slightly larger than the predicted 24.6 kDa size of the recombinant protein. Bands exhibiting migration patterns consistent with the size of AbmR dimers (just larger than 48 kDa) and higher order oligomers were detected by western blot with anti-AbmR serum in glutaraldehyde cross-linked samples (Fig. 1D). These results support AbmR oligomerization and a prediction in the Doodle database (https://oligomers.tamu.edu/) that AbmR is likely to self-associate. The multi-banded pattern of cross-linked AbmR oligomers was also strikingly similar to the multi-banded shift pattern observed in DNA binding EMSA experiments (Fig. 1B). Oligomerization in these experiments was observed

in dilute protein samples with 150 mM NaCl and low glutaraldehyde concentrations, suggesting that the observed oligomers were not artifacts of excessive cross-linking or non-specific charged-based interactions.

Analytical ultracentrifugation (AUC) was used to further monitor the oligomerization of AbmR in solution at different concentrations. AbmR was found in three major populations with s20, w values of 2.7 s, 39 s and 58 s (Fig. 1E and F). To determine whether AbmR was forming high molecular weight aggregates, we negatively stained AbmR and examined the protein using transmission electron microscopy (TEM). Surprisingly, AbmR was found to form regular, organized high molecular weight complexes (Fig. 1G). These organized complexes were maintained with the addition of 570 mM NaCl (Fig. S6C) but were not observed when the C-terminus of AbmR was truncated (Fig. S6D). These data further support our initial conclusion that AbmR oligomerizes in solution, and that this activity requires the C-terminus of AbmR.

Localization of AbmR *binding*

We further defined the region of DNA needed for AbmR binding by testing which contiguous sequences were required to observe a band shift by EMSA. Purified AbmR bound a DNA probe covering the entire region between the end of the *Rv1264* ORF and the beginning of the *abmR* ORF (Probe 1 in Fig. 2B and C). No AbmR

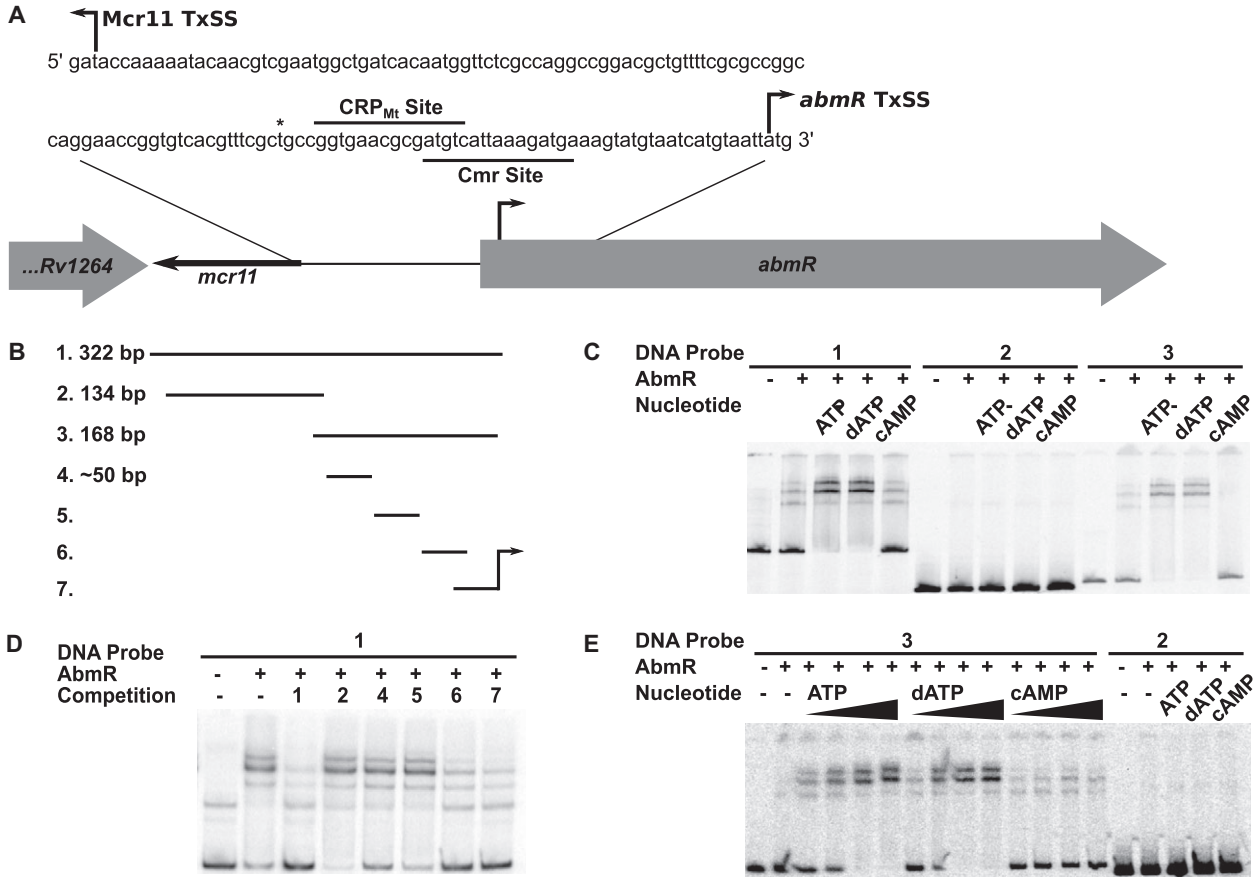

Fig. 2. AbmR DNA-binding activity is enhanced by the addition of d/ATP, but not cAMP.
A. The *mcr11-abmR* locus is illustrated, with previously reported transcriptional start sites for each gene indicated by a bent arrow. The DNA sequence spanning the *mcr11-abmR* intergenic space is shown in detail, with previously reported CRP$_{Mt}$- and Cmr-binding sites indicated by a line. An asterisk (*) marks the 5′ end of Probe 6 shown in part (B).
B. Labeled DNA probes used for EMSAs are indicated by numbered black lines and the size of the DNA probe is listed to the left.
C. The effect of 5 mM ATP, dATP or cAMP on the DNA-binding activity of 1.5 μM of AbmR and the indicated DNA probes was tested by EMSA.
D. Unlabeled DNA competitor fragments are indicated by numbered lines and correspond to the position of DNA probes shown in (B). Competitor fragments overlapped with each other by 3–19 base pairs and competitor fragments 4–7 were ~ 50 base pairs in size. For reference, the position of the AbmR transcriptional start is marked with a bent arrow. A competition EMSA with Probe 1, 5 mM ATP, 1.5 μM of AbmR and 250-fold excess unlabeled DNA competitor.
E. The dose-dependent effect of ATP and dATP on DNA binding of probe 3 was tested with 1.5 μM of AbmR and nucleotide concentrations ranging from 0.5 to 10 mM. DNA probe 2 with or without 10 mM of the indicated nucleotide was used as a negative control. Results representative of three independent experiments.

binding was observed when the probe consisted only of the DNA region spanning from the end of the *Rv1264* ORF through the *mcr11* gene (Probe 2 in Fig. 2B and C). In contrast, AbmR bound the intergenic DNA region between *mcr11* and *abmR* (Probe 3 in Fig. 2B and C). Using competition EMSAs to better localize AbmR binding, we observed that unlabeled DNA competitor fragments 6 and 7, but not 4 or 5, successfully competed for AbmR binding (Fig. 2D). These results localize AbmR binding to a 75-base pair DNA region that includes previously reported Cmr and CRP_{Mt} binding sites (Gazdik *et al*., 2009; Arnvig *et al*., 2011) as well as the transcriptional start site of *abmR* (Fig. 2A) (Gazdik *et al*., 2009; Cortes *et al*., 2013). Unlabeled Probe 1 was used as a positive competition control and unlabeled Probe 2 was used as a negative control (Fig. 2D). From this, we conclude that AbmR binds a DNA sequence proximal to the transcriptional start sites of both the *mcr11* and *abmR* genes.

DNA-binding activity of AbmR *responds to d/ATP*

AbmR expression is upregulated in the presence of cAMP (Gazdik and McDonough, 2005), so we tested the effects of cAMP and ATP on AbmR's DNA-binding activity. cAMP did not alter the DNA binding of AbmR, but the addition of ATP or dATP enhanced AbmR binding of Probes 1 and 3 (Fig. 2C and E). Both ATP and dATP increased AbmR binding of DNA Probe 3 in a dose-dependent manner, whereas cAMP had no significant effect at any concentration tested (Fig. 2E). AbmR did not bind Probe 2, even in the presence of 10 mM ATP, dATP or cAMP. These results establish that the *in vitro* DNA-binding activity of recombinant AbmR is enhanced in a concentration-dependent manner by the addition of ATP or dATP, but not cAMP, and that this effect is specific to the DNA ligand.

AbmR *directly and specifically binds d/ATP*

The effects of d/ATP on AbmR's DNA-binding activity suggested that AbmR directly interacts with d/ATP, and we reasoned that AbmR could be engaging in auto-phosphorylation using ATP as a substrate. The ability of AbmR to interact with d/ATP in the presence of different divalent cations was tested by native gel electrophoresis. Recombinant AbmR interacted with γ-^{33}P-ATP or α-^{32}P-dATP only when a divalent cation such as Ca^{2+}, Mg^{2+} or Mn^{2+} was present (Figs 3A and S2C). All tested concentrations of Mg^{2+} equally supported interaction with ATP, whereas Ca^{2+} and Mn^{2+} facilitated interaction with ATP only at a concentration of 5 mM (Fig. 3A). Interaction of AbmR with dATP appeared less robust than with ATP regardless of divalent cation concentration (Fig. S2C). AbmR's interaction with radiolabeled ATP was competed away by excess cold ATP or dATP, but not cAMP, in the presence of 5 mM divalent cation (Fig. 3B). We further tested the ability of cAMP to compete for ATP binding by adding excess cAMP prior to adding radiolabeled ATP to AbmR. Even in vast excess, cAMP did not compete for ATP binding by AbmR (Fig. S2A). These data demonstrate that AbmR directly and specifically interacts with d/ATP rather than cAMP.

Next, we tested whether AbmR was covalently interacting with ATP by evaluating the retention of radiolabeled ATP by denatured AbmR. When AbmR:ATP-binding

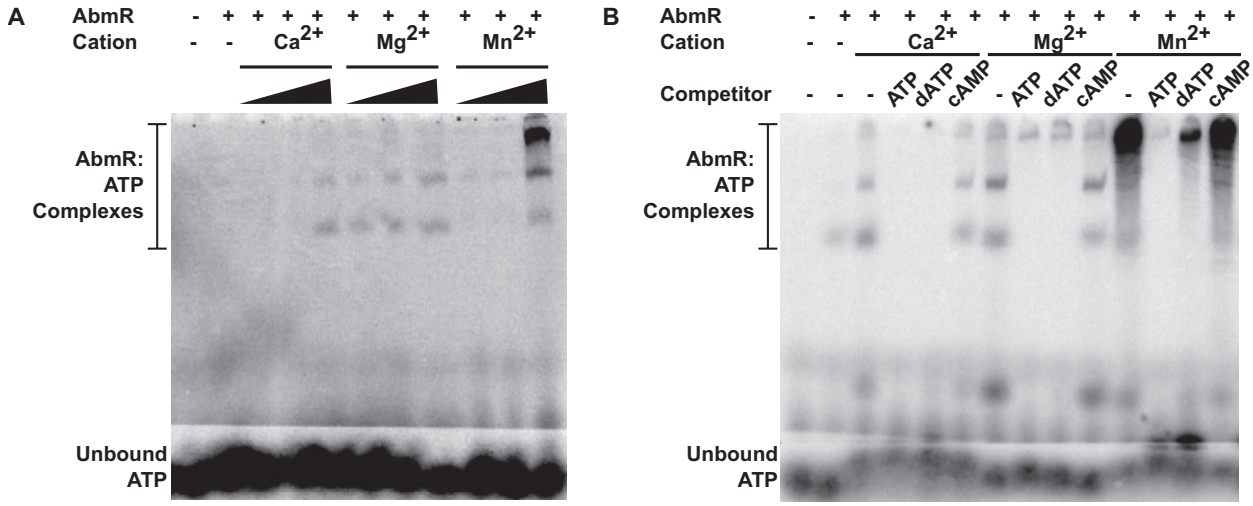

Fig. 3. AbmR directly and specifically binds ATP.
A. The ability of AbmR to bind γ-^{33}P-ATP was tested by EMSA. 10 μM of recombinant AbmR was added to γ-^{33}P-ATP in the presence of 0.5 mM, 1 mM or 5 mM of the indicated bivalent cation.
B. The specificity of AbmR's ATP-binding activity was tested using a competition EMSA. 10 μM of recombinant AbmR was added to γ-^{33}P-ATP in the presence of 5 mM of the indicated bivalent cation, with and without 500-fold excess unlabeled nucleotide competitors. Results representative of three independent experiments.

reactions were exposed to denaturing conditions during SDS-PAGE, the radiolabeled γ-^{33}P-ATP was observed at the dye front, separate from the protein band observed in a duplicate Coomassie Brilliant Blue-stained gel (Fig. S2B). Thus, we conclude that AbmR's interaction with ATP is non-covalent. Addition of 5 mM ATP, dATP or cAMP failed to alter the oligomerization status of AbmR in cross-linked samples, demonstrating that oligomerization is independent of nucleotide binding (Fig. S2D).

AbmR *is an auto-repressor and activator of mcr11 expression*

We generated knockout mutants of *abmR* in BCG and Mtb using homologous recombination (Fig. S3A and C) to study its biological function. Many TFs engage in auto-regulation, so we measured the promoter activities of *abmR* (P*abmR*) and the divergent gene *mcr11* (P*mcr11*) using GFP Venus (GFPv) reporter fusions in wild type (Wt) or *abmR*-deleted (MtbΔ*abmR*) strains of Mtb (Fig. 4A). *Mcr11* expression has been shown to be responsive to growth phase (Arnvig *et al*., 2011; DiChiara *et al*., 2010; Pelly *et al*., 2012), so we also measured promoter activities across growth phase while determining the role of *abmR* in their regulation.

Expression from P*mcr11* was reduced in MtbΔ*abmR* relative to Wt in all growth phases tested (Fig. 4B–D). While P*mcr11* activity significantly increased with advancing growth phase in Wt Mtb, no activation of P*mcr11* was observed in MtbΔ*abmR* (Fig. 4D). These results suggest that AbmR up-regulates *mcr11* expression in response to growth phase. Conversely, P*abmR* activity was 6–11-fold greater in MtbΔ*abmR* than in Wt cells (Fig.e 4B, C and E), indicating auto-repression. The magnitude of P*abmR* de-repression in MtbΔ*abmR* increased between mid-log and stationary growth phases (p = 0.0017, Fig. 4E). Promoterless vector-only containing strains were used as negative controls and showed low levels of fluorescence. Positive control promoter fusions for *tuf* and *pknA* exhibited no differences in activity between Wt versus MtbΔ*abmR* (Fig. 4B and C). Mutant and recombinant strains grew similarly to Wt controls (data not shown).

qRT-PCR analysis was performed to further evaluate the effect of *abmR* deletion on gene expression in Mtb. As observed with promoter:reporter fusions, Mcr11 expression was reduced in MtbΔ*abmR* relative to Wt bacteria in both mid-log phase and late stationary phase (Fig. 5A). Complementation of *abmR* in single copy restored Mcr11 abundance to Wt levels (Compl. 1, Fig. 5A). As this construct includes the native *abmR* promoter with contiguous *mcr11* DNA sequences, we also measured Mcr11 expression in a multi-copy complementation vector with *abmR* under the control of a non-native promoter (Compl. 2). Complementation of the *abmR* deletion with the multi-copy expression vector also restored Mcr11 abundance to Wt levels (Compl. 2, Fig. 5A). Northern blot analysis

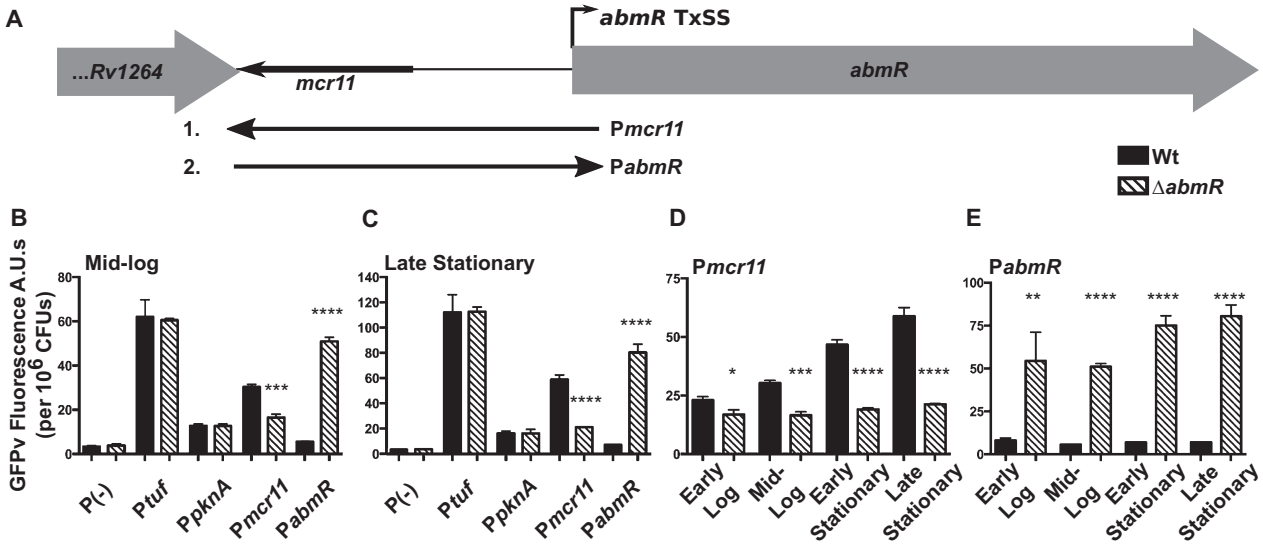

Fig. 4. AbmR activates expression of the ncRNA Mcr11 and auto-represses expression of *abmR* in Mtb. A. Black arrows indicated the DNA sequence used in the *mcr11* promoter:*GFPv* fusion (1.) and the *abmR* promoter:*GFPv* fusion (2.). Promoter:*GFPv* reporter analysis was conducted in hypoxia (1.3% O_2, 5% CO_2) with wild-type and MtbΔ*abmR* across growth phases. B. Results of mid-log phase and C. late stationary phase reporter assays are shown. Promoterless (P(-)) and *abmR*-independent positive controls (P*tuf*, P*pknA*) were included. C. Growth-phase dependent activation of Pmcr11 was assayed using a *mcr11* promoter:*GFPv* fusion reporter in Mtb . Y-axis label shown applies to graphs in (B–E). E. P*abmR* activity was monitored by GFPv fluorescence across growth phase in Wt and MtbΔ*abmR*. Results are the mean values from three independent experiments. Statistical analysis conducted with an unpaired, 2-tailed Student's *t*-test. Asterisks indicate when MtbΔ*abmR* was significantly different than wild type as follows: $^{*}p < 0.05$, $^{**}p < 0.01$, $^{***}p < 0.001$, $^{****}p < 0.0001$.

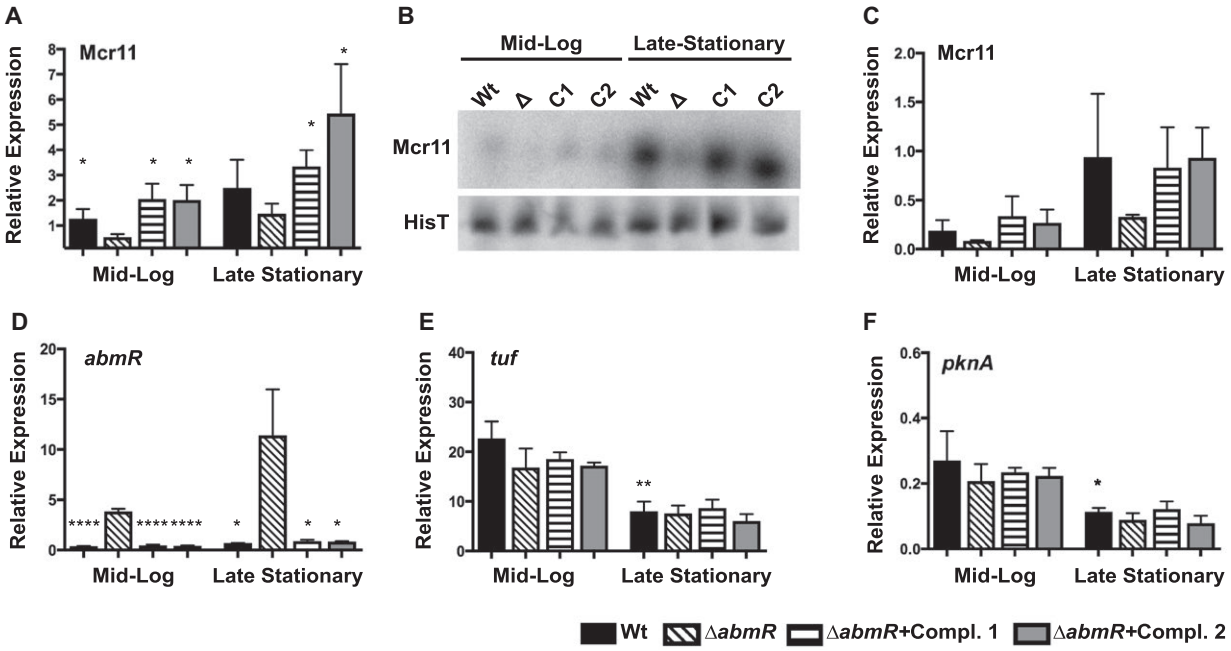

Fig. 5. Complementation of AbmR restores *mcr11* and *abmR* expression levels in Mtb. A. qRT-PCR analysis of Mcr11 expression levels of mid-log and late stationary phase Wt Mtb grown in hypoxia (1.3% O_2, 5% CO_2) was compared to Mtb*ΔabmR* and *abmR* complementation in single (Compl. 1) or multiple (Compl. 2) copies. B. Northern blot analysis of Mcr11 expression levels of mid-log and late stationary phase Wt Mtb compared to Mtb*ΔabmR* and *abmR* complementation in single (C1) or multiple (C2) copies. HisT is used as a loading control. C. Densitometry analysis of Mcr11 expression assayed by northern blot. D. qRT-PCR analysis of 5'*abmR* expression. The expression of *tuf* (E.) and *pknA* (F.) control genes was assayed by qRT-PCR. Expression normalized to sigA (A, C–D) or HisT (B) levels. Results are the means three independent experiments. Statistical analysis conducted with an unpaired, 2-tailed Student's *t*-test. Asterisks indicate when a strain was significantly different than Mtb*ΔabmR* (A and D) or in Wt mid-log phase versus Wt stationary phase (E and F) as follows: $^{*}p < 0.05$, $^{**}p < 0.01$, $^{***}p < 0.001$, $^{****}p < 0.0001$.

of Mcr11 levels yielded similar results (Fig. 5B and C), further demonstrating that *abmR* positively regulates expression of the sRNA Mcr11.

The Δ*abmR* mutants were generated in such a way that a portion of the uninterrupted 5′ end of *abmR* mRNA could be detected in Δ*abmR* cDNA (Fig. S3A). Thus, we compared relative levels of native P*abmR* activity in mutant versus Wt Mtb by qRT-PCR with primers designed to amplify the most 5′ end of the *abmR* gene. Expression from the native *abmR* promoter increased approximately 5–10-fold in Mtb*ΔabmR* compared to Wt, and complementation of *abmR* in single or multiple copies restored *abmR* expression to Wt levels (Fig. 5D). These results support the conclusion that AbmR represses its own expression. Control levels of *tuf* and *pknA* mRNAs were unaltered in Mtb*ΔabmR*, although significant downregulation of both genes was observed in late stationary phase compared to mid-log phase (Fig. 5E and F).

De-repression of *abmR* expression was also observed by promoter:reporter activity assays and by qRT-PCR in BCG*ΔabmR* versus Wt BCG (Fig. S4A and C). Similarly, Mcr11 transcript levels were generally reduced in BCG*ΔabmR* (Fig. S4B). From these data, we conclude that *abmR* exerts its function as a positive regulator of *mcr11* and a repressor of *abmR* expression in BCG as well as Mtb.

Point mutagenesis of AbmR alters DNA binding and gene regulation

The results above demonstrate that AbmR is a DNA-binding protein that regulates expression of *mcr11* and *abmR*. We sought to establish whether AbmR's DNA-binding activity is required for this regulatory function by using point mutagenesis to strategically replace amino acids in the predicted nucleic acid binding region. Alignments of the AbmR amino acid sequences of Mtb and BCG yielded proteins with 99.47% identity and similarity, while the *Mycobacterium smegmatis* (Msm) orthologue of AbmR has 68.75% identity and 83.51% similarity to AbmR in Mtb (Fig. 6A). The web-based DNA- and RNA-binding site prediction tool BindN (https://bioinformatics.ksu.edu/bindn/) (Wang and Brown, 2006) predicted with high confidence a conserved pair of nucleic acid-interacting arginine residues in the putative nucleic acid binding region of AbmR (data not shown). Examination of these arginines in the Phyre[2] top hit Protein Data Bank file using PyMOL Molecular Graphics System (Version 1.8 Schrödinger, LLC) suggested that R146 is available to contact nucleic acid and that R148 is involved in forming a salt bridge that helps maintain the conformation of the structural motif (Fig. 6B).

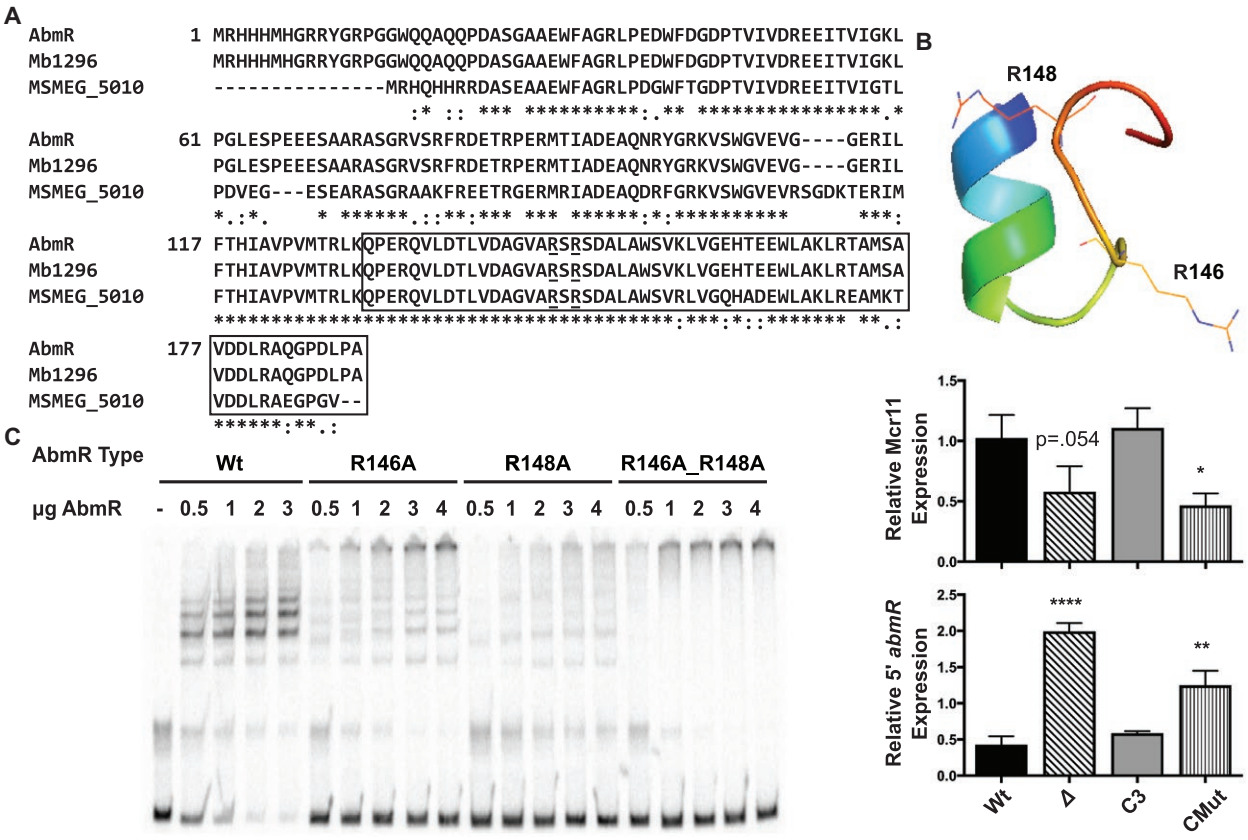

Fig. 6. The DNA-binding activity of AbmR is required for the gene regulatory function of *abmR in vivo*.
A. Clustal Omega alignments of the BCG (Mb1296) and Msm (MSMEG_5010) are aligned to Mtb AbmR. An asterisk (*) indicates positions with a single, conserved residue. Colons (:) indicate conservation between groups with strongly similar properties and periods (.) indicate conservation between groups with weakly similar properties. Arginines 146 and 148 are underlined in black. The predicted nucleic acid-binding domain is outlined in a black box.
B. A simplified diagram of the predicted fold of AbmR that aligns to top Phyre[2] hit (SCOPe fold d1h3fa2), with arginines 146 and 148 shown as line drawings and indicated by bolded text.
C. EMSA analysis of the DNA-binding activity of the indicated point mutants for a DNA probe of the *mcr11-abmR* intergenic region in the presence of 5 mM ATP is shown. Representative of three independent repeats. qRT-PCR comparing the expression of Mcr11 and *abmR* in Wt, Mtb*ΔabmR* (Δ), a single-copy complement overexpressing *abmR* (C3) and a single-copy complement strain overexpressing *abmR* with the R146A point mutation (CMut). Results are the means of three biological replicates. Statistical analysis conducted with an unpaired, 2-tailed Student's *t*-test. Asterisks indicate when a strain was significantly different than Mtb*ΔabmR* (Mcr11) or Wt (5′ *abmR*) as follows: $^{*}p < 0.05$, $^{**}p < 0.01$, $^{***}p < 0.001$.

Both arginines were mutagenized individually and in combination to examine their impacts on the DNA-binding activity of AbmR. All three mutant versions of AbmR self-associated normally in cross-linked western blot analyses, indicating that none were grossly mis-folded (Fig. S5A). Furthermore, the R146A mutant AbmR formed high molecular weight complexes in solution similar to those of wild-type protein (Fig. S6B). In the presence of 5 mM ATP, both R146A and R148A demonstrated greatly diminished ability to bind a DNA probe of the *mcr11-abmR* intergenic region (Fig. 6C). The DNA-binding activity of R146A_R148A was negligible and poorly resolved (Fig. 6C). Similarly, single-point mutants of AbmR retained significant ATP-binding capacity in the presence of Mn^{2+}, whereas the double-point mutant and the mutant with the truncated predicted nucleic acid-binding region bound ATP poorly (Fig. S5B). From these data, we conclude that R146 and R148 are critical for the DNA-binding activity of AbmR.

An AbmR R 146A overexpression plasmid (CMut) was transformed into Mtb*ΔabmR* to evaluate the impact of this mutation on the gene regulatory function of *abmR* (Fig. S5C). The AbmR R1446A-complemented strain of Mtb*ΔabmR* behaved similarly to Mtb*ΔabmR* mutant with respect to regulation of *abmR* and *mcr11* expression in Mtb grown shaking to late stationary phase under hypoxic conditions (Figs 6D and S5C). These data show that R146, which is required for optimal DNA-binding activity *in vitro*, is also required for the gene regulatory function of AbmR *in vivo*. Thus, we conclude that *abmR* encodes

a novel ATP-responsive transcription factor with gene regulatory function that is dependent on its DNA-binding activity.

Macrophage infection and survival

After determining the biochemical function of AbmR, we explored additional biological roles of AbmR that may contribute to Mtb pathogenesis. Expression of *abmR* is upregulated early after macrophage infection (Hobson *et al*., 2002; Gazdik *et al*., 2009), so survival of Mtb*ΔabmR* in murine macrophages was compared to Wt and complemented controls. BCG*ΔabmR* displayed a mild sensitivity to treatment with nitric oxide (data not shown), so the ability of Mtb*ΔabmR* to survive in activated murine macrophages was also tested.

Approximately 2-fold fewer Mtb*ΔabmR* bacteria were recovered from resting and activated J774.1 murine macrophages at 4 h post-infection compared to Wt or single-copy *abmR*-complemented strains (Fig. S7A and B). However, approximately twice as many Mtb*ΔabmR* bacteria were recovered versus Wt or complemented strains at 1d post-infection (Figs S7A and B). Consequently, the change in bacterial burden from 4 h to 1 d was 2.5–6-fold greater in macrophages infected with Mtb*ΔabmR* compared to Wt or *abmR* complement-infected macrophages (Fig. 7A). Growth and survival of Mtb*ΔabmR* within macrophages was unaltered at later time points (Fig. S7A and B). Strong overexpression of *abmR* resulted in a significant growth-delay in both Wt and BCG*ΔabmR* strains (Fig. 7B), further suggesting *abmR* could have a role in negatively regulating the growth of slow-growing mycobacteria. These data indicate *abmR* is not required to survive within resting or activated macrophages. However, the results suggest *abmR* may be involved in host cell entry and/or bacterial replication immediately following initial host cell entry.

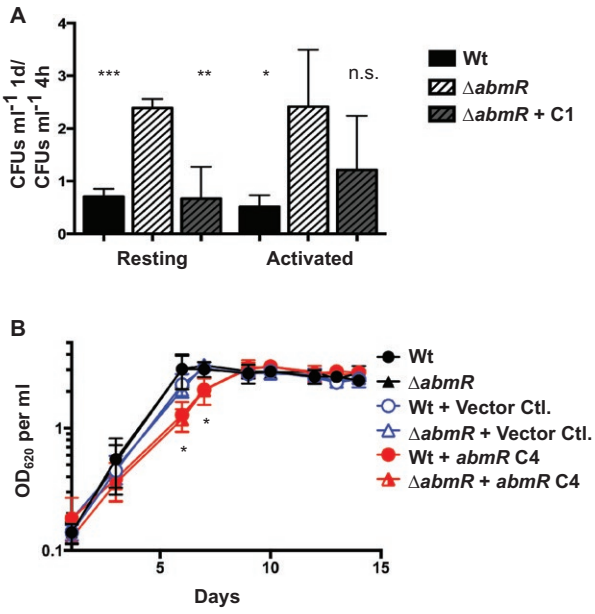

Fig. 7. *abmR* is not required for survival in murine macrophages, but may have a role in negatively regulating growth.
A. Analysis of the fold change of CFUs recovered from resting or LPS and IFN-γ activated J774.16 murine macrophages after 1 d of infection versus 4h of infection with Wt, Mtb*ΔabmR* or single-copy *abmR*-complemented strains.
B. Growth of wild-type (Wt) and BCG*ΔabmR* strains with an empty complementation vector (Vector Ctl.), or a single-copy strong *abmR* overexpression vector (*abmR* C4) was monitored by measuring the OD at 620 nm. Statistical analysis was conducted with an unpaired, 2-tailed Student's *t*-test. Asterisks indicate when a strain was significantly different from Mtb*ΔabmR* (in panel A) or both *abmR* overexpression strains (in panel B).

Invasion assay

Mtb can enter macrophages through multiple host-dependent pathways (McDonough *et al*., 1993; Schlesinger, 1993; Zimmerli *et al*., 1996; Schorey *et al*., 1997; Bermudez and Sangari, 2001; Velasco-Velazquez *et al*., 2003), and we reasoned that non-phagocytic host cells could serve as a model for studying bacterial determinants of host cell invasion. The ability of Mtb*ΔabmR* to invade cultured human lung epithelial A549 cells was compared in Wt- and *abmR*-complemented controls. Serum has been shown to contribute to the ability of *Mycobacterium* species to invade host cells (McDonough and Kress, 1995; Schorey *et al*., 1997), so these assays were conducted in the presence of FBS, heat-inactivated FBS or in serum-free media.

The presence of serum significantly increased the percentage of epithelial cells containing acid-fast bacilli (AFB) and the infectivity index of Wt Mtb (Supplemental Table 3). Relative to Wt, Mtb*ΔabmR* infected 1.7–3.8-fold fewer epithelial cells and exhibited a 2.3–4.3-fold decreased infectivity index in the presence of serum (Fig. 8A and B). The magnitude of the host cell association deficit of Mtb*ΔabmR* varied depending on the serum lot used (Supplemental Table 3). The number of bacteria per infected epithelial cell was similar in Wt and Mtb*ΔabmR* samples (Fig. 8C). Bacteria appeared to be intracellular, rather than adherent, consistent with previous results (McDonough and Kress, 1995). Complementation of *abmR* restored Wt levels of host cell association in the presence of serum (Fig. 8A and B). There was no difference in levels of host cell association between Wt and Mtb*ΔabmR* in the absence of serum or in the presence of heat-inactivated serum (Fig. S8B–D). Input colony-forming units (CFUs) were similar across strains and inocula type (Fig. S8A). Thus, we concluded that *abmR* facilitates Mtb's association with A549 lung epithelial cells through a heat-labile serum component.

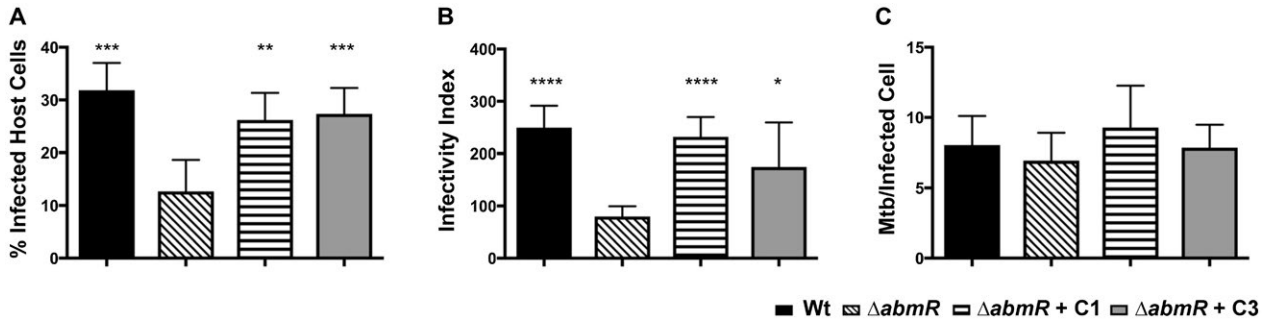

Fig. 8. *abmR* is required for adherence to and invasion of A549 epithelial cells.
A. Percentage of A549 epithelial cells scored as positive for acid-fast bacilli after 2 h of infection in the presence of 10% FBS.
B. The infectivity index (number of Mtb/100 host cells) of each strain after 2 h of infection in the presence of 10% FBS.
C. Number of acid-fast bacilli (Mtb) per infected A549 epithelial cell. Strains included Wt, Mtb*ΔabmR* or single-copy *abmR*-complemented strains (C1 and C3). Results are the means of six independent experiments. Statistical analysis conducted with an unpaired, 2-tailed Student's *t*-test. Asterisks indicate when a strain was significantly different than Mtb*ΔabmR* as follows: $^{*}p < 0.05$, $^{**}p < 0.01$, $^{***}p < 0.001$, $^{****}p < 0.0001$.

Heparin-binding haemagglutinin adhesin (HBHA, gene *Rv0475*), is required for adhesion to epithelial cells and extrapulmonary dissemination (Menozzi *et al.*, 1996; Pethe *et al.*, 2001), so RNA and protein were harvested from Mtb for HBHA expression analysis. Transcript levels of *hbha* were unaltered in Mtb*ΔabmR*, as measured by qRT-PCR (Fig. S8E), and comparable levels of HBHA were detected in all strains by western blot analysis (Fig. S8F). Thus, the host cell invasion deficit of Mtb*ΔabmR* is not due to a loss of HBHA expression.

Discussion

AbmR *is a novel transcription factor*

This study showed that AbmR binds both ATP and DNA, while directly regulating the expression of itself and that of the sRNA Mcr11. These findings were unexpected because AbmR does not share obvious sequence similarity with other well-characterized DNA- or ATP-binding domains. A secondary structure-based bioinformatic prediction of protein function provided a critical breakthrough for our discovery that the conserved hypothetical gene *abmR* encodes a DNA-binding protein. Structure-based bioinformatics analyses were also essential for guiding mutagenesis studies that established the importance of amino acids R146 and R148 for AbmR's DNA-binding activity and gene expression regulatory function. Together, these findings emphasize the value of bioinformatics in combination with structure-based modeling as a tool for characterizing genes of unknown function.

The DNA-binding properties and gene regulatory functions of AbmR implicate it as a previously undescribed transcription factor (TF) that may respond to cellular ATP levels. Detailed structural information on AbmR will be required to further characterize the domain organization and mechanism by which AbmR binds DNA. Helix–turn–helix and ribbon–helix–helix folds account for the DNA-binding properties of the vast majority of characterized prokaryotic transcription factors (Schreiter and Drennan, 2007; Seshasayee *et al.*, 2011). The limited homology with other known DNA-binding proteins suggests that AbmR may have a novel domain distantly related to currently described DNA-binding protein domains. True protein domains are defined as tertiary structural elements with a hydrophobic core that can evolve and function independently of the rest of the protein. It is not clear whether the C-terminus of AbmR can independently fold into such a stable nucleic acid-binding element, or simply comprises a specialized motif within a larger functional domain. In either case, the unexpected identification of AbmR's biochemical functions raises the possibility that Mtb's genome encodes additional, unrecognized TFs.

Biochemical features of AbmR

The ribbon–helix–helix domain of a CopG-like protein (Gomis-Ruth *et al.*, 1998) was a top Phyre[2] hit for the predicted nucleic acid-binding region of AbmR, and the two proteins share a number of biochemical features despite their limited homology. CopG, a transcriptional repressor protein that regulates plasmid copy number, is known for its oligomerization, multi-banded EMSA super shifts and bending of DNA at an operator sequence flanked by A-rich tracts (Gomis-Ruth *et al.*, 1998). Future work is needed to determine whether there are also functional parallels between AbmR and CopG. Three of the four structural predictions for nucleic acid-binding motifs in the C-terminus of AbmR were based on alpha-L RNA-binding motifs. Although we did not observe RNA-binding activity for AbmR, AbmR may also have an uncharacterized RNA-binding function, as reported for some

eukaryotic DNA- and RNA-binding proteins (Hudson and Ortlund, 2014).

AbmR self-associates to form dimers and higher order oligomers, a feature common to many TFs. The EMSA super-shift pattern observed with AbmR may reflect binding of DNA by AbmR oligomers. However, AbmR oligomerized in the absence of added DNA ligand, suggesting that oligomerization is not occurring on DNA as it does with EthR repressor complexes in Mtb (Engohang-Ndong *et al*., 2003). This conclusion is further supported by the observation that point replacement of amino acids critical for the optimal DNA-binding activity of AbmR did not adversely affect the oligomerization of AbmR. The biological significance of the large, organized particles that AbmR forms in solution is unknown. Future studies are needed to determine which species of AbmR oligomers are involved in DNA binding and whether AbmR is also capable of bending DNA ligands.

Multi-banded super-shift patterns in EMSAs are often observed with TFs that bind non-specific or degenerate motifs (Murray *et al*., 2006; Chen *et al*., 2008; Lewis, 2011). For example, CmtR, a cadmium-sensing repressor of Mtb, forms high-order multimers and binds an AT-rich DNA sequence (Chauhan *et al*., 2009). The presence of Cd(II) disrupts the CmtR interaction with DNA and allows for de-repression of the *cmtR-Rv1993c-cmtA* operon (Chauhan *et al*., 2009). The specific DNA sequences bound by AbmR in its operator are currently under investigation, with several repeated sequences and tracts of unusually low GC content being of interest.

Many TFs bind effector molecules such as nucleotides, and a plethora of adenosine nucleotide-binding proteins, have been identified in Mtb (Ansong *et al*., 2013). While cAMP had no effect on AbmR's DNA-binding activity, ATP increased DNA-binding activity substantially. Phosphotransfer from ATP to AbmR was not observed, nor was hydrolysis of ATP. Thus, our data indicate that ATP is a ligand of AbmR rather than a substrate. AbmR was not identified as an ATP-binding protein by previous experimental approaches (Ansong *et al*., 2013; Wolfe *et al*., 2013), although the absence of AbmR from these reports could be due to low expression levels of *abmR* in the growth conditions tested. The wide diversity of mycobacterial proteins found to have ATP-binding function (Ansong *et al*., 2013) suggests the presence of other as-yet uncharacterized ATP-binding domains in Mtb. Elucidation of the structural features of AbmR's ATP-binding activity is thus likely to lead to identification of an additional novel protein domain.

Several families of TFs experience conformational rearrangements upon binding of cofactors that alter the TF's affinity for DNA ligands (Bueno *et al*., 2012). It is possible that AbmR undergoes a similar conformational shift upon binding ATP that enhances its affinity for the binding site in the *mcr11-abmR* intergenic region. Sensing and responding to fluctuations in ATP levels has an established role in the pathogenesis of other bacteria (Lee and Groisman, 2012) and is thought to contribute to virulence gene regulation (Zhang *et al*., 2014) and bacteriocidal stress response in Mtb (Koul *et al*., 2014). Decreased cellular ATP levels in Mtb occur during non-replicating persistence (NRP) (Wayne and Hayes, 1996; Rao *et al*., 2008; Gengenbacher *et al*., 2010), while regulation of ATP synthesis and the electron transport chain is associated with adaptation to the macrophage, the mouse lung, hypoxia and dormancy (Wayne and Sohaskey, 2001; Schnappinger *et al*., 2003; Voskuil *et al*., 2004; Shi *et al*., 2005; Garton *et al*., 2008; Shi *et al*., 2010). Evaluation of AbmR's role in ATP signaling networks and the survival of Mtb during NRP could further understanding of a critical component of TB pathogenesis.

abmR *contributes to host cell association*

It was recently reported that overexpression of *abmR* enhanced survival of Msm exposed to stress and within host cells (Luo *et al*., 2016). However, we did not observe large defects in BCGΔ*abmR* survival after treatment with nitric oxide, low pH or cell wall stress (data not shown) and MtbΔ*abmR* displayed no survival defect in resting or activated murine macrophages. Rather, an increase in MtbΔ*abmR* CFUs in early in macrophage infection was observed despite a lower initial bacterial burden. In addition, Wt and BCGΔ*abmR* constitutively overexpressing *abmR* experience a significant growth lag *in vitro*. AbmR could have a role as a negative growth regulator, which could contribute to survival in the host during NRP. Overexpression of the ATP-binding universal stress protein (USP) Rv2623 also causes a growth lag of Mtb *in vitro* (Drumm *et al*., 2009); the ATP-binding activities of AbmR and Rv2623 could contribute to the observed growth delays upon overexpression. Alternatively, the observed growth delays may be a downstream effect of the ncRNA Mcr11. Constitutive overexpression of Mcr11 has been associated with growth lag in Mtb (Ignatov *et al*., 2015), although the direct targets of Mcr11 regulation have not been identified.

AbmR likely mediates the serum-dependent adherence and/or invasion of non-phagocytic lung epithelial cells through factors other than the adhesin HBHA, as we did not observe changes in HBHA expression that could account for this phenotype. Multiple additional proteins have been shown to mediate the attachment of Mtb to lung epithelial cells, some of which are unique to TB complex mycobacteria (Mueller-Ortiz *et al*., 2002; Reddy and Hayworth, 2002; Vidal Pessolani *et al*., 2003; Ramsugit *et al*., 2016). While we did not observe dysregulation of these factors at the mRNA level (data not shown), the

abundance of these proteins may be altered at the translational level by ncRNAs (such as Mcr11) regulated by AbmR. Alternatively, AbmR may directly interact with host cells in a serum-dependent manner. The surface exposed, DNA-binding protein HupB, encoded by gene *Rv2986c*, mediates host cell attachment of Mtb to epithelial cells (Aoki *et al*., 2004). AbmR has been recovered from the membrane fraction of Mtb, so it may also directly interact with host cells, similar to HupB (Malen *et al*., 2010; de Souza *et al*., 2011; Gu *et al*., 2003). Characterization of the cell surface and proteome of Mtb Δ*abmR* will further our understanding of bacterial factors that mediate host cell adherence and invasion of Mtb.

Gene regulatory functions of AbmR *and regulatory networks*

Our finding that AbmR engages in auto-repression and growth phase-responsive activation of *mcr11* expression is consistent with the location of AbmR binding in the operator region shared by both genes. The mechanism by which AbmR engages is auto-repression is unknown, but we reason that binding of AbmR at its operator could result in simultaneous auto-repression and activation of the divergently transcribed sRNA Mcr11 during hypoxia. Future work will be needed to determine if AbmR exerts its gene regulatory functions through direct interaction with RNA polymerase, or if one or more protein partners are required.

cAMP levels are associated with regulation of both AbmR and Mcr11 levels and adaptation to the host environment (Gazdik and McDonough, 2005; Pelly *et al*., 2012). *AbmR*'s putative operator contains a biochemically validated Cmr-binding site (Gazdik *et al*., 2009) and a predicted CRP_{Mt}-binding site (Arnvig *et al*., 2011). While neither TF was found within the *Rv1264-mcr11-abmR* region in recent ChIP-seq studies (Kahramanoglou *et al*., 2014, Knapp *et al*., 2015; Ranganathan *et al*., 2016), regulation of *abmR* by both Cmr and CRP_{Mt} have been reported (Gazdik *et al*., 2009; Arnvig *et al*., 2011; Kahramanoglou *et al*., 2014; Knapp *et al*., 2015). The possibility that AbmR, Cmr and/or CRP_{Mt} engage in competitive or cooperative DNA binding in this region warrants further investigation, as does the potential for indirect regulation by AbmR of gene targets downstream of Mcr11.

Recent work has demonstrated that AbmR is phosphorylated by multiple ATP-dependent serine/threonine protein kinases (Wu *et al*., 2017), including the kinase downstream of AbmR, PknH (*Rv1266c*). The functional impact of post-translational modification (PTM) of AbmR by phosphorylation is unknown, but PTM of AbmR may feed into an ATP sensing and signaling network. PknH has a demonstrated role in phosphorylating the dormancy survival response regulator (DosR) (Chao *et al*., 2010), and regulatory overlaps between DosR and Cmr have recently been revealed (Ranganathan *et al*., 2016; Smith *et al*., 2017). Decrypting the regulatory overlap of AbmR and cAMP responsive TFs such as CRP_{Mt} and Cmr during infection and persistence will contribute to our understanding of Mtb's adaptation to the host environment.

These findings identify a CHP as a novel auto-inhibitory TF that regulates expression of itself and an sRNA associated with growth arrest in Mtb (Pelly *et al*., 2012; Ignatov *et al*., 2015). They also demonstrate the power of secondary structure-based bioinformatic tools that leverage experimentally derived structural data for generating testable hypotheses when seeking to characterize genes of unknown function. Further study of the structural features and regulatory targets of AbmR will provide important new insights into the unique biology of Mtb and advance our understanding of this deadly pathogen.

Experimental procedures

Bacterial strains and growth conditions

Mycobacterium tuberculosis H37Rv (Mtb) (ATCC 25618) was grown on 7H10 agar (Difco) supplemented with 10% oleic acid-albumin-dextrose-catalase (OADC) (Becton Dickson and Company) and 0.01% cycloheximide or in Middlebrook 7H9 liquid medium (Difco) supplemented with 10% (vol/vol) OADC, 0.2% (vol/vol) glycerol, 10% (vol/vol) and 0.05% (vol/vol) Tween-80 (Sigma-Aldrich). *Mycobacterium bovis* BCG (BCG) (Pasteur strain, Trudeau Institute) was grown in similar media, but with 10% (vol/vol) albumin-dextrose-catalase (Becton Dickson and Company) instead of OADC. Cultures were grown to various growth phases in gently shaking vented 25-cm^2 tissue culture flasks (Corning) in low oxygen (1.3% O_2, 5% CO_2) for gene expression experiments (Florczyk *et al*., 2001). For analysis of the impact of substitution of R144A in AbmR on gene expression, Mtb was grown to late stationary phase in shaking, hypoxic conditions. Each experiment was started from low-passage frozen stocks. *Escherichia coli* strains were grown on Luria-Bertani (Difco) agar plates or in liquid broth. Media was supplemented with 50 μg ml^{-1} hygromycin, 25 μg ml^{-1} kanamycin (Sigma-Aldrich) or 35 μg ml^{-1} chloramphenicol (Sigma-Aldrich) as appropriate. Cultures were incubated at 37°C unless otherwise detailed.

Mutant strain construction

abmR knockout strains of BCG and Mtb were generated using homologous recombination to replace codons 66 through 86 with a hygromycin resistance cassette. The upstream and downstream flanking sequences of *abmR* were amplified with primers KM1170, KM1171, KM2075

and KM2076 and cloned into pMBC851 (Bai *et al*., 2011). This plasmid was digested with PacI and ligated with PacI digested phAE159 plasmid vector (Bardarov *et al*., 2002) and *abmR* was knocked out as previously described (Bai *et al*., 2011). Deletion was confirmed by polymerase chain reaction (PCR) and western blot analysis (Fig. S3C). Multi-copy and single-copy *abmR* expression constructs were created to complement Δ*abmR strains*. The *abmR* ORF and a portion of the corresponding intergenic region upstream of *abmR* excluding *mcr11* was PCR amplified with primers KM2784 and KM2659 and cloned downstream of the *tuf* (*Rv0685*) promoter into multi-copy expression vector pMBC283 (Bai *et al*., 2011), which contains a kanamycin resistance cassette, to create pMBC1117. An integrating complementation construct was generated by PCR amplifying sequence from the end of the *Rv1264* ORF through the end of the *abmR* ORF with primers KM2658 and KM2659 and cloning into pMBC409, which contains a kanamycin resistance marker, to create pMBC1070. Single copy *abmR* overexpression vectors were created by PCR amplifying the intergenic region upstream of *abmR* excluding *mcr11* using primers KM3586 and KM3498 and cloned downstream of the *tuf* promoter in pMBC1258 (which is derived from pMBC 409 and contains a kanamycin resistance marker) to create pMBC1583. A single-copy strong overexpression vector was created by PCR amplifying the region from the corrected start site of the *abmR* ORF through the annotated end and using primers KM3497 and KM3498 cloning in downstream of the *tuf* promoter in pMBC1258 to create pMBC1729. Complementation plasmids were sequence verified and used to transform Mtb and BCG by electroporation.

Cloning, expression and purification of recombinant AbmR

Promoter:reporter fusion studies, homology searches (Gazdik *et al*., 2009) and transcriptional start site mapping (Cortes *et al*., 2013) all support the re-annotation of the AbmR ORF start site to a methionine 38 amino acids downstream of the start codon reported in Tuberculist (Lew *et al*., 2011). Thus, we used this corrected 190 amino acid AbmR ORF, which starts 112 nucleotides downstream of the annotated start site, for our experiments. The corrected AbmR ORF polypeptide sequence (Gazdik *et al*., 2009) was modeled using Protein Homology/analog Recognition Engine V 2.0 (Phyre^2) (Kelley and Sternberg, 2009). Following modeling, N-terminal His6x tagged recombinant AbmR was created by amplifying the corrected *abmR* ORF from genomic Mtb DNA and cloning the PCR product into the BamHI and EcoRI sites in pET28a+ (Novagen) to create pMBC1571. AbmR with the predicted nucleic acid-binding region truncated after amino acid 130 was similarly PCR amplified and cloned into pET28a+ to create pMBC1565. Expression constructs were sequence verified and maintained in Rosetta^{tm} (DE3)pLysS *E. coli* (Novagen).

Bacterial cultures were expanded to optical density (OD) at 600 nM of 0.5–0.6 and then AbmR expression was induced by the addition of 1 mM isopropyl-β-thio-galactopyranoside (MBP Biomedicals) for 24 h at 15°C. Recombinant protein was purified from 0.5 L of induced cells that were pelleted and resuspended in 12.5 ml of lysis buffer containing 50 mM Tris-HCl pH 8.0, 10% (vol/vol) glycerol, 1 mM dithiothreitol (DTT) (Sigma-Aldrich) and 0.02% (vol/vol) protease inhibitor cocktail (Sigma-Aldrich). Cells were disrupted by sonication in a Virsonic 475 Ultrasonic Cell Disrupter with a cup horn attachment (VirTis Company) chilled to 4°C. Lysates were raised to 25 ml with the addition of 5 mM $MgCl_2$ and DNaseI (New England Biolabs) and DNA digestion was carried out at room temperature for 30 min. Cell debris was pelleted and cleared lysate was raised to 50 ml with the addition of 0.5 M NaCl and 50 mM imidazole (Sigma-Aldrich). Lysate was passed sequentially through 5 µM and 0.45 µM Minisart NML syringe filters (Sartorius) before purification using a HisTrap HP (GE Healthcare Life Sciences) nickel-charged column on an AKTA Prime Plus (GE Healthcare Life Sciences). Protein was eluted with a shallow imidazole gradient and collected in fractions. Fractions containing the desired purified recombinant protein were extensively dialyzed into 20 mM 4-(2-hydroxyethyl)-1-piperazineethanesulfonic acid (HEPES) pH 8.0 with 150 mM NaCl or 20 mM Tris-HCl pH 8.0 with 10% (vol/vol) glycerol storage buffer with 0.1 M sucrose as needed.

Electrophoretic mobility shift assays

Electrophoretic mobility shifty assays (EMSAs) were performed as described previously with modification (Bai *et al*., 2005). ^{33}P-end-labeled DNA probes (0.05 pmol) (primers listed in Table S1) were incubated with 1.5 µM recombinant AbmR in DNA binding buffer (10 mM Tris-HCl pH 9.0, 50 mM KCl, 1 mM EDTA, 50 µg ml^{-1} BSA, 1 mM DTT, 0.05% NP-40, 20 µg ml^{-1} poly dI-dC and 10% (vol/vol) glycerol) at room temperature for 30 min. DNA-binding reactions contained 5 mM ATP unless otherwise noted. Nucleotide dose-dependent experiments were performed with 0.5, 1, 5 and 10 mM ATP, dATP or cAMP. Predicted nucleic acid-binding region truncated AbmR was added in increasing concentrations from 2 to 8 µM. For competition experiments, 250-fold excess unlabeled DNA fragments were used. The ORF of *sigA* was used as a non-specific competitor. DNA-binding reactions were resolved on a non-denaturing 8% (weight/vol) polyacrylamide gel run for 2.5 h, 14 V/cm at 4°C in 0.5x Tris-borate-EDTA (TBE), pH

9.0. RNA EMSAs were performed with 1.5 μM recombinant AbmR in RNA binding buffer (10 mM Tris-HCl, pH 8.0, 50 mM NaCl, 50 mM KCl, 10 mM $MgCl_2$, 10% (vol/vol) yeast tRNA) with ^{33}P-end-labeled RNA probes (0.2 pmol) generated by T7 or Sp6 RNA polymerase run-off transcription from linearized plasmid template (listed in Table S1) as previously described (Zhang *et al*., 2002). RNA-binding reactions were incubated at 37°C for 15 min and then 10x loading dye (1x TBE, 50% (vol/vol) glycerol, 0.1% (weight/vol) bromophenol blue, 0.1% (weight//vol) xylene cyanol) was added and reactions were resolved on a non-denaturing 6% (weight/vol) polyacrylamide gel run at 4°C in 0.5x TBE. EMSAs were visualized with a Storm 860 PhosphorImager (Molecular Dynamics).

ATP- and dATP-binding experiments were similarly completed, but 0.042 μM γ-^{33}P-ATP or α-^{32}P-dATP was incubated with 10 μM recombinant AbmR in DNA-binding buffer in the presence or absence of divalent cations. Divalent cations were added at 0.5 mM, 1 mM and 5 mM in dose-dependent experiments and at 5 mM for competition experiments. Five hundred-fold excess unlabeled nucleotides were used in competition experiments. Binding reactions were resolved on a non-denaturing 6% (weight/vol) polyacrylamide gel or by SDS-PAGE. Interactions with radiolabeled nucleotides were visualized with a Storm 860 PhosphorImager (Molecular Dynamics) and recombinant protein was visualized by staining with Coomassie Brilliant Blue (CBB).

Oligomerization analysis

Database of oligomerization domains from lambda experiments (Doodle), maintained by the Hu Lab at Texas A&M (Marino-Ramirez *et al*., 2004), was accessed on 09/24/14 and was searched for hits in the *abmR* ORF. The database indicated AbmR might oligomerize, so the ability of purified recombinant AbmR to self-associate was tested *in vitro*. Briefly, 500 nm was cross-linked with 0.0025–0.025% (vol/vol) glutaraldehyde in cross-linking buffer (20 mM HEPES pH 8.0, 150 mM NaCl, 5 mM $MgCl_2$ 10% (vol/vol) glycerol) with or without 5 mM nucleotide for 30 min at room temperature. Cross-linking was quenched with SDS-PAGE loading buffer and samples were separated by SDS-PAGE. The presence of oligomers was ascertained by western blotting with anti-AbmR serum as described below.

Analytical ultracentrifugation

The properties of recombinant AbmR in 20 mM HEPES, pH 8.0 with 150 mM NaCl were investigated by AUC. Sedimentation velocity experiments were carried out in an Optima XL-I analytical ultracentrifuge (Beckman) at 4°C and a rotor speed of 10,000 rpm. Samples were loaded in double-sector charcoal-filled epon centerpieces in an AN-60 Ti four-hole rotor. Absorption measurements were made at 280 nm with zero time between scans. All samples were compared to a dialysis buffer only reference cell, and the centrifuge and rotor were maintained at thermal equilibrium for at least 1 h before experiments were initiated. Data were analyzed using the c(s) method found in SEDFIT (Schuck, 2000), and vbar, density and viscosity were calculated using SEDNTERP. Experimentally determined sedimentation coefficients were calculated using the c(s) method and converted to s20, w values within the SEDFIT software and graphed using Prizm 5 (GraphPad).

Electron microscopy

Recombinant AbmR at a concentration of 0.75 mg ml^{-1} in 20 mM HEPES, pH 8.0 with 150 mM NaCl was thawed on ice, and then mixed 5:1 (protein:gold) with a concentrated solution of 10 nm gold particles (Sigma Aldrich). Three microliters of sample were then placed on copper 300 mesh grids (Ted Pella) and incubated at room temperature for 1 min, then rinsed gently with deionized water. Excess liquid was removed with filter paper and 3 μl of 0.1 mM NaCl solution was added to the grid, incubated for 45 s and then filter paper was used to remove excess liquid. Finally, samples were stained with 3% uranyl acetate for 1 min, and excess liquid was removed with filter paper. Each sample was then examined on a JEM-1400 Plus transmission electron microscope (JEOL USA) at 80 kV and images were captured at 100,000x magnification.

Generation of mycobacterial cell lysates

Late-log phase bacteria were harvested and washed twice in an equal volume of chilled Dulbecco's phosphate buffered saline, calcium- and magnesium-free (DPBS-CMF), with 0.2% protease inhibitor (Sigma-Aldrich). Bacterial pellets were resuspended in lysis buffer (0.3% SDS, 200 mM DTT, 28 mM Tris-HCl, 22 mM Tris-Base and 1% protease inhibitor cocktail) 1/25 of the original culture volume. Cells were lysed with two rounds sonication using a Virsonic 475 Ultrasonic Cell Disrupter with a cup horn attachment (VirTis Company), with 10 freeze–thaw cycles interspersed between sonication rounds. Cell debris was removed by centrifugation and the cleared lysate was heat-killed for 10 min at 95°C. Protein in the cleared lysates was quantified using the NanoOrange® Protein Quantitation Kit (Molecular Probes) and the NanoDrop 2000 (Thermo Scientific).

Western blotting

Cell lysates or recombinant AbmR samples were separated by 4.5% stacking and 15% resolving Tris-glycine SDS-PAGE. CBB staining of duplicate gels was used to check the evenness of sample loading. Gels were immunoblotted on Immobilon-P membranes (Millipore) for 1 h at 1 mA cm^{-2} using a wet transfer system (Bio-Rad Laboratories). Blocking was achieved in 5% non-fat milk in 50 mM Tris-buffered saline with 0.05% (vol/vol) Tween-20 (Fisher Scientific). The following reagents were obtained through the NIH Biodefense and Emerging Infections Research Resources Repository, NIAID, NIH: Monoclonal Anti-*Mycobacterium tuberculosis* HBHA (Gene Rv0475), Clone α-HBHA (produced *in vitro*) and NR-13804 and monoclonal Anti-*Mycobacterium tuberculosis* GlcB (Gene Rv1837c), Clone α-GlcB (produced *in vitro*). Polyclonal AbmR anti-serum was generated *in vivo* by immunizing three specific pathogen-free 4–8 week old female BALB/c mice (Taconic Biosciences) three times biweekly with 10 µg of recombinant AbmR diluted in alum. The serum was pooled and the specificity of the AbmR anti-serum was confirmed by western blotting with recombinant AbmR and by observing the absence of a band of the expected size in the *abmR* mutant strain. Primary antibodies were detected with peroxidase conjugated goat anti-mouse secondary antibody and enhanced chemiluminescence (ECL) western blotting detection reagent (Thermo Scientific).

Promoter:reporter gene construction

Promoter regions of various positive expression controls (*tuf*, *pknA/B*) and test genes (*mcr11*, *abmR*) were PCR amplified using the primers listed in Table S1 and cloned into the BamHI site of pMBC1798. pMBC1798 contains a Shine–Dalgarno site followed by green fluorescent protein Venus (GFPv) ORF adjacent to the BamHI site on the plasmid backbone pMBC304, which contains a kanamycin resistance gene and an integration cassette and. Promoter:*GFPv* reporter fusion plasmids were sequence verified and used to transform wild-type and mutant Mtb and BCG by electroporation.

Promoter:reporter fusion assay

At desired time points, aliquots of recombinant Mtb or BCG cultures were collected and sonicated briefly using a Virsonic 475 Ultrasonic Cell Disrupter with a cup horn attachment (VirTis Company) before duplicate samples were diluted in fresh media. The OD at 620 nm was read using a Tecan Sunrise® microplate reader. The level of fluorescence from the GFPv reporter gene was detected using the CytoFluor Multi-Well Plate Reader Series 4000 (PerSeptive Biosystems) at 485 nm excitation and 530 nm emission. Fluorescence levels were normalized to 10^6 bacteria as determined by OD at 620 nm. A promoterless vector-only *GFPv* strain was included as a negative control.

RNA isolation and quantitative RT-PCR

Liquid cultures of BCG or Mtb were treated with 0.5 M final GTC solution (5.0 M guanadinium isothiocyanate, 25 mM sodium citrate, 0.5% sarkosyl and 0.1 M 2-β-mercaptoethanol) and pelleted at 4°C. Cell pellets were resuspended in TRIzol Reagent (Invitrogen) and 0.1 mm zironia–silica beads (BioSpec Products) were added. The bacteria were mechanically disrupted with three 70 s high-speed pulses in a bead-beater (BioSpec Products). Total RNA was extracted from cell lysate using Direct-zol Mini Prep columns (Zymo) per the manufacturer's protocol. RNA was eluted in DNA and RNAse free-water and treated with DNaseI (Qiagen) for 30 min at room temperature, and then isopropanol precipitated. One microgram of total RNA was screened for DNA contamination by PCR using primers KM1309 and KM1310 for the *sigA* ORF. RNA quality was assessed by running 1.0 µg of DNA-free RNA on an agarose gel containing 0.1% (weight/vol) SDS and visualizing intact 23S, 16S and 5S ribosomal RNA bands after staining with ethidium bromide (Sigma-Aldrich).

cDNA was prepared using 1.0 µg DNA and RNAse free total RNA and 0.125 µg of random primers RPA00, RPT00, RPC00 and RPG00 as previously described (Gazdik *et al*., 2009). One microliter of a 1:5 dilution of cDNA was used in a 10 µl qPCR reaction containing 0.3 µM of each primer and iTAQ Universal SYBR® Green Supermix (BioRad). Real-time PCR analysis was performed using an ABI Prism® 7000 Sequence Detection System (Applied Biosysytems) at 1 cycle of 50°C for 2 min, 1 cycle of 95°C for 10 min and 40 cycles of 95°C for 15 s, 60°C for 1 min. Relative gene expression calculated using the $2^{-\Delta Ct}$ method, with the reference gene sigA (Livak and Schmittgen, 2001). All primer sets are listed in Table S1 and were subjected to quality analysis prior to use in assays. Relative expression of *abmR* was divided by 2 in complemented strains to account for the second copy of the 5′ end of the *abmR* ORF available in the complement (Fig. S3A).

Northern blots

Approximately 5.0 µg of DNA- and RNAse-free total RNA was separated on a 10% 8 M urea PAGE run at a constant current of 15 mA for 1.5 h. The gel was then electroblotted onto a Hybond N (Millipore) nylon membrane using a wet transfer system (Bio-Rad Laboratories). Blots

were UV cross-linked and baked at 80°C for 2 h prior to pre-hybridization at 42°C for 4 h as previously described (DiChiara *et al*., 2010). Hybridization with α-^{32}P-ATP end-labeled DNA oligo probes was performed at 42°C overnight. Blots were washed with 2X SSC (0.3 M NaCl, 30 mM trisodium citrate, pH 7.0), 0.1% (weight/vol) SDS at 65°C until background was low and then exposed to phosphor screens for visualization.

Point mutagenesis of AbmR

Alignment of the amino acid sequences of AbmR and the BCG and *Mycobacterium smegamtis* (Msm) orthologs was completed using Clustal Omega (EMBL-EBI). Absolutely conserved amino acids in the predicted nucleic acid-binding region were considered for mutagenesis. The BindN web-based tool was used to predict the probability of a conserved residue's ability to contact and interact favorably with nucleic acid (Wang and Brown, 2006). After examining the position of candidate residues within the top Phyre2 hit (SCOPe fold d1h3fa2), arginines at positions 146 and 148 were selected for mutagenesis. Mutagenesis was accomplished with sequence overlap extension with the primers listed in Table S1, as previously described (Vasudeva-Rao and McDonough, 2008). Sequence verified point mutant versions of AbmR were and cloned into the BamHI and EcoRI sites in pET28a+ (Novagen) and transformed into Rosetta^{tm} (DE3)pLysS *E. coli* (Novagen) to create strains pMBC1691 (R146A), pMBC1802 (R148A) and pMBC1690 (R146A_R148A). Recombinant proteins were purified and used for EMSA and western blot analysis as described previously.

AbmR was cloned into the KpnI and BamHI restriction sites in the mycobacterial single-copy integrating expression vector pMBC1258, which allowed for expression of *abmR* from a copy of the *tuf* (*Rv0685*) promoter and kanamycin resistance selection (pMBC1583). QuikChange Site-Directed Mutagenesis (Agilent) was used to introduce the R146A point mutation into pMBC1583 according to the manufacturer's protocol to create pMBC1805. This plasmid was electroporated into MtbΔ*abmR*, and positive transformants were confirmed by PCR and western blot analysis.

Host cell infections

J774.16 murine macrophages were seeded at 2×10^5 cells/well in DMEM supplemented with 20% (vol/vol) fetal bovine serum (FBS) in six-well microtiter dishes 12–16 h prior to infection. Macrophages were activated with 500 U ml^{-1} of IFN-γ for 16 h prior to infection, and monolayers were infected with DMEM supplemented with 20% (vol/vol) FBS, 500 U ml^{-1} IFN-γ and 1 µg ml^{-1} lipopolysaccharide (LPS) (Chan *et al*., 1992). Macrophage monolayers were infected for 4 h with Wt, MtbΔ*abmR* or MtbΔ*abmR*::pMBC1070 at a multiplicity of infection (MOI) of 1:1 as described previously (Gazdik *et al*., 2009). The inoculum was removed and infected monolayers were washed thrice with Dulbecco's phosphate-buffered saline (DPBS) to remove extracellular bacteria. Infected macrophages were maintained in fresh DMEM with 20% FBS at 37°C. The monolayer was lysed with 0.5% deoxycholate (weight/vol), 0.5% Triton X-100 (vol/vol) in calcium- and magnesium-free DPBS at the indicated time points. Lysates were sonicated briefly as described (McDonough and Kress, 1995) and serially diluted in DPBS with 0.05% Tween-80 before plating for enumeration of CFUs on 7H10 agar (Difco) supplemented with 10% OADC and 0.01% cyclohexamide. CFUs were recorded after 4 weeks of incubation at 37°C.

The human lung pneomocyte A549 cell line (CCL 185) was seeded onto glass coverslips at 5×10^5 cells/well in Ham's F12 medium supplemented with 10% (vol/vol) FBS 12–16 h prior to infection. Monolayers were washed three times in condition-specific media prior to infection. A549 cells were infected at an MOI of 200:1 for 2 h in Ham's F12 medium supplemented with 10% (vol/vol) FBS, 10% (vol/vol) heat-inactivated FBS (HI-FBS) or in serum-free Ham's F12 medium. Two different lots of serum were used for three biological repeats each for the normal serum condition. Serum-free and heat-inactivated serum experiments were conducted three times. The inoculum was removed and the infected monolayer was washed thrice with DPBS to remove extracellular bacteria. Infected monolayers were fixed with 4% paraformaldehyde in DPBS for 30 min at room temperature. Fixed coverslips were rinsed in DPBS and stained with Kinyoun acid-fast stain. Using a light microscope, 100–400 cells per slide were scored for presence of AFB. The percentage of AFB positive host cells, the number of bacteria per AFB positive host cell and the number of bacteria per 100 cells (infectivity index) were determined (McDonough and Kress, 1995).

Acknowledgements

We thank Damen Schaak for his role in generating Mtb *abmR* knockout and complementation strains used in this study. We are also very grateful for the assistance of Karen Chave, who provided invaluable guidance during early efforts to purify recombinant AbmR, Drs. Joe Jaeger and Janice Pata, who helped us visualize and interpret bioinformatic models in PyMol and Leslie Eisele for additional technical assistance. We further acknowledge the Wadsworth Center Applied Genomics Technologies Core for DNA sequencing, the Tissue Culture and Media Core for media preparation, the Biochemistry and Immunology

core for analytical ultracentrifugation and the Electron Microscopy core for imaging.

This work was supported in part by National Institutes of Health grants R01AI063499 and R01AI045658 to KAM. RCG was supported by National Institute of Allergy and Infectious Disease training grant T32AI055429.

Author Contributions

RCG and KAM conceived experiments. RCG, GB and JH performed experiments or generated materials. RCG, KAM and HXS analyzed and interpreted data. RCG and KAM wrote the manuscript.

References

Agarwal, N., Lamichhane, G., Gupta, R., Nolan, S. and Bishai, W.R. (2009) Cyclic AMP intoxication of macrophages by a *Mycobacterium tuberculosis* adenylate cyclase. *Nature*, **460**, 98–102.

Ansong, C., Ortega, C., Payne, S.H., Haft, D.H., Chauvigne-Hines, L.M., Lewis, M.P., *et al*. (2013) Identification of widespread adenosine nucleotide binding in *Mycobacterium tuberculosis*. *Chemistry & Biology*, **20**, 123–133.

Aoki, K., Matsumoto, S., Hirayama, Y., Wada, T., Ozeki, Y., Niki, M. *et al*. (2004) Extracellular mycobacterial DNA-binding protein 1 participates in mycobacterium-lung epithelial cell interaction through hyaluronic acid. *The Journal of Biological Chemistry*, **279**, 39798–39806.

Arnvig, K.B., Comas, I., Thomson, N.R., Houghton, J., Boshoff, H.I., Croucher, N.J. *et al*. (2011) Sequence-based analysis uncovers an abundance of non-coding RNA in the total transcriptome of *Mycobacterium tuberculosis*. *PLoS Pathogen*, **7**, e1002342.

Arnvig, K.B. and Young, D.B. (2009) Identification of small RNAs in *Mycobacterium tuberculosis*. *Molecular Microbiology*, **73**, 397–408.

Bai, G., McCue, L.A. and McDonough, K.A. (2005) Characterization of *Mycobacterium tuberculosis* Rv3676 (CRPMt), a cyclic AMP receptor protein-like DNA binding protein. *Journal of Bacteriology*, **187**, 7795–7804.

Bai, G., Schaak, D.D. and McDonough, K.A. (2009) cAMP levels within *Mycobacterium tuberculosis* and *Mycobacterium bovis* BCG increase upon infection of macrophages. *FEMS Immunology and Medical Microbiology*, **55**, 68–73.

Bai, G., Schaak, D.D., Smith, E.A. and McDonough, K.A. (2011) Dysregulation of serine biosynthesis contributes to the growth defect of a *Mycobacterium tuberculosis* crp mutant. *Molecular Microbiology*, **82**, 180–198.

Banerjee, S.K., Kumar, M., Alokam, R., Sharma, A.K., Chatterjee, A., Kumar, R. *et al*. (2016) Targeting multiple response regulators of *Mycobacterium tuberculosis* augments the host immune response to infection. *Scientific reports*, **6**, 25851.

Bardarov, S., Bardarov, S. Jr., Pavelka, M.S. Jr., Sambandamurthy, V. Jr., Larsen, M., Tufariello, J. (2002) Specialized transduction: an efficient method for generating marked and unmarked targeted gene disruptions in *Mycobacterium tuberculosis*, M. bovis BCG and M. smegmatis. *Microbiology*, **148**, 3007–3017.

Bermudez, L.E. and Sangari, F.J. (2001) Cellular and molecular mechanisms of internalization of mycobacteria by host cells. *Microbes and Infection*, **3**, 37–42.

Betts, J.C., Lukey, P.T., Robb, L.C., McAdam, R.A. and Duncan, K. (2002) Evaluation of a nutrient starvation model of *Mycobacterium tuberculosis* persistence by gene and protein expression profiling. *Molecular Microbiology*, **43**, 717–731.

Bueno, E., Mesa, S., Bedmar, E.J., Richardson, D.J. and Delgado, M.J. (2012) Bacterial adaptation of respiration from oxic to microoxic and anoxic conditions: redox control. *Antioxidants & redox signaling*, **16**, 819–852.

Camus, J.-C., Pryor, M.J., Médigue, C. and Cole, S.T. (2002) Re-annotation of the genome sequence of *Mycobacterium tuberculosis* H37Rv. *Microbiology*, **148**, 2967–2973.

Chan, J., Xing, Y., Magliozzo, R.S. and Bloom, B.R. (1992) Killing of virulent *Mycobacterium tuberculosis* by reactive nitrogen intermediates produced by activated murine macrophages. *The Journal of Experimental Medicine*, **175**, 1111–1122.

Chao, J.D., Papavinasasundaram, K.G., Zheng, X., Chavez-Steenbock, A., Wang, X., Lee, G.Q. *et al*. (2010) Convergence of Ser/Thr and two-component signaling to coordinate expression of the dormancy regulon in *Mycobacterium tuberculosis*. *The Journal of Biological Chemistry*, **285**, 29239–29246.

Chauhan, S., Kumar, A., Singhal, A., Tyagi, J.S. and Krishna Prasad, H. (2009) CmtR, a cadmium-sensing ArsR-SmtB repressor, cooperatively interacts with multiple operator sites to autorepress its transcription in *Mycobacterium tuberculosis*. *The FEBS Journal*, **276**, 3428–3439.

Chen, J.M., Ren, H., Shaw, J.E., Wang, Y.J., Li, M., Leung, A.S. *et al*. (2008) Lsr2 of *Mycobacterium tuberculosis* is a DNA-bridging protein. *Nucleic Acids Research*, **36**, 2123–2135.

Cole, S.T., Brosch, R., Parkhill, J., Garnier, T., Churcher, C., Harris, D. *et al*. (1998) Deciphering the biology of *Mycobacterium tuberculosis* from the complete genome sequence. *Nature*, **393**, 537–544.

Cortes, T., Schubert, O.T., Rose, G., Arnvig, K.B., Comas, I., Aebersold, R., *et al*. (2013) Genome-wide mapping of transcriptional start sites defines an extensive leaderless transcriptome in *Mycobacterium tuberculosis*. *Cell Reports*, **5**, 1121–1131.

de Souza, G.A., Leversen, N.A., Malen, H. and Wiker, H.G. (2011) Bacterial proteins with cleaved or uncleaved signal peptides of the general secretory pathway. *Journal of Proteomics*, **75**, 502–510.

DiChiara, J.M., Contreras-Martinez, L.M., Livny, J., Smith, D., McDonough, K.A. and Belfort, M. (2010) Multiple small RNAs identified in *Mycobacterium bovis* BCG are also expressed in *Mycobacterium tuberculosis* and *Mycobacterium smegmatis*. *Nucleic Acids Research*, **38**, 4067–4078.

Doerks, T., van Noort, V., Minguez, P. and Bork, P. (2012) Annotation of the *M. tuberculosis* hypothetical orfeome: adding functional information to more than half of the uncharacterized proteins. *PLoS One*, **7**, e34302.

Drumm, J.E., Mi, K., Bilder, P., Sun, M., Lim, J., Bielefeldt-Ohmann, H. *et al*. (2009) *Mycobacterium tuberculosis* universal stress protein Rv2623 regulates bacillary growth by ATP-Binding: requirement for establishing chronic persistent infection. *PLoS Pathogen*, **5**, e1000460.

Du, P., Sohaskey, C.D. and Shi, L. (2016) Transcriptional and physiological changes during *Mycobacterium tuberculosis* reactivation from non-replicating persistence. *Frontiers in Microbiology*, **7**, 1346.

Engohang-Ndong, J., Baillat, D., Aumercier, M., Bellefontaine, F., Besra, G.S., Locht, C., *et al*. (2003) EthR, a repressor of the TetR/CamR family implicated in ethionamide resistance in mycobacteria, octamerizes cooperatively on its operator. *Molecular Microbiology*, **51**, 175–188.

Flentie, K., Garner, A.L. and Stallings, C.L. (2016) *Mycobacterium tuberculosis* transcription machinery: ready to respond to host attacks. *Journal of Bacteriology*, **198**, 1360–1373.

Florczyk, M.A., McCue, L.A., Stack, R.F., Hauer, C.R. and McDonough, K.A. (2001) Identification and characterization of mycobacterial proteins differentially expressed under standing and shaking culture conditions, including Rv2623 from a novel class of putative ATP-binding proteins. *Infection and Immunity*, **69**, 5777–5785.

Galagan, J.E., Minch, K., Peterson, M., Lyubetskaya, A., Azizi, E., Sweet, L. *et al*. (2013) The *Mycobacterium tuberculosis* regulatory network and hypoxia. *Nature*, **499**, 178–183.

Garton, N.J., Waddell, S.J., Sherratt, A.L., Lee, S.M., Smith, R.J., Senner, C. *et al*. (2008) Cytological and transcript analyses reveal fat and lazy persister-like bacilli in tuberculous sputum. *PLoS medicine*, **5**, e75.

Gautam, U.S., Mehra, S. and Kaushal, D. (2015) In-Vivo Gene Signatures of *Mycobacterium tuberculosis* in C3HeB/FeJ Mice. *PLoS One*, **10**, e0135208.

Gazdik, M.A., Bai, G., Wu, Y. and McDonough, K.A. (2009) Rv1675c (cmr) regulates intramacrophage and cyclic AMP-induced gene expression in *Mycobacterium tuberculosis*-complex mycobacteria. *Molecular Microbiology*, **71**, 434–448.

Gazdik, M.A. and McDonough, K.A. (2005) Identification of cyclic AMP-regulated genes in *Mycobacterium tuberculosis* complex bacteria under low-oxygen conditions. *Journal of Bacteriology*, **187**, 2681–2692.

Gengenbacher, M., Rao, S.P., Pethe, K. and Dick, T. (2010) Nutrient-starved, non-replicating *Mycobacterium tuberculosis* requires respiration, ATP synthase and isocitrate lyase for maintenance of ATP homeostasis and viability. *Microbiology*, **156**, 81–87.

Gomis-Ruth, F.X., Sola, M., Acebo, P., Parraga, A., Guasch, A., Eritja, R. *et al*. (1998) The structure of plasmid-encoded transcriptional repressor CopG unliganded and bound to its operator. *The EMBO Journal*, **17**, 7404–7415.

Goodacre, N.F., Gerloff, D.L. and Uetz, P. (2014) Protein domains of unknown function are essential in bacteria. *MBio*, **5**, e00744–00713.

Gu, S., Chen, J., Dobos, K.M., Bradbury, E.M., Belisle, J.T. and Chen, X. (2003) Comprehensive proteomic profiling of the membrane constituents of a *Mycobacterium tuberculosis* strain. *Molecular & Cellular Proteomics*, **2**, 1284–1296.

Hobson, R.J., McBride, A.J., Kempsell, K.E. and Dale, J.W. (2002) Use of an arrayed promoter-probe library for the identification of macrophage-regulated genes in *Mycobacterium tuberculosis*. *Microbiology*, **148**, 1571–1579.

Hudson, W.H. and Ortlund, E.A. (2014) The structure, function and evolution of proteins that bind DNA and RNA. *Nature Reviews Molecular Cell Biology*, **15**, 749–760.

Ignatov, D.V., Salina, E.G., Fursov, M.V., Skvortsov, T.A., Azhikina, T.L. and Kaprelyants, A.S. (2015) Dormant non-culturable *Mycobacterium tuberculosis* retains stable low-abundant mRNA. *BMC Genomics*, **16**, 954.

Iona, E., Pardini, M., Mustazzolu, A., Piccaro, G., Nisini, R., Fattorini, L. *et al*. (2016) *Mycobacterium tuberculosis* gene expression at different stages of hypoxia-induced dormancy and upon resuscitation. *Journal of microbiology (Seoul, Korea)*, **54**, 565–572.

Johnson, R.M., Bai, G., DeMott, C.M., Banavali, N.K., Montague, C.R., Moon, C. *et al*. (2017) Chemical activation of adenylyl cyclase Rv1625c inhibits growth of *Mycobacterium tuberculosis* on cholesterol and modulates intramacrophage signaling. *Molecular Microbiology*, **105**, 294–308.

Kahramanoglou, C., Cortes, T., Matange, N., Hunt, D.M., Visweswariah, S.S. Young, D.B. *et al*. (2014) Genomic mapping of cAMP receptor protein (CRP Mt) in *Mycobacterium tuberculosis*: relation to transcriptional start sites and the role of CRPMt as a transcription factor. *Nucleic Acids Research*, **42**, 8320–8329.

Kelley, L.A. and Sternberg, M.J. (2009) Protein structure prediction on the Web: a case study using the Phyre server. *Nature Protocols*, **4**, 363–371.

Knapp, G.S., Lyubetskaya, A., Peterson, M.W., Gomes, A.L., Ma, Z., Galagan, J.E. *et al*. (2015) Role of intragenic binding of cAMP responsive protein (CRP) in regulation of the succinate dehydrogenase genes Rv0249c-Rv0247c in TB complex mycobacteria. *Nucleic Acids Research*, **43**, 5377–5393.

Koul, A., Vranckx, L., Dhar, N., Gohlmann, H.W., Ozdemir, E., Neefs, J.M. *et al*. (2014) Delayed bactericidal response of *Mycobacterium tuberculosis* to bedaquiline involves remodelling of bacterial metabolism. *Nature Communications*, **5**, 3369.

Lamichhane, G., Zignol, M., Blades, N.J., Geiman, D.E., Dougherty, A., Grosset, J. *et al*. (2003) A postgenomic method for predicting essential genes at subsaturation levels of mutagenesis: application to *Mycobacterium tuberculosis*. *Proceedings of the National Academy of Sciences of the United States of America*, **100**, 7213–7218.

Lee, E.J. and Groisman, E.A. (2012) Control of a *Salmonella* virulence locus by an ATP-sensing leader messenger RNA. *Nature*, **486**, 271–275.

Lew, J.M., Kapopoulou, A., Jones, L.M. and Cole, S.T. (2011) TubercuList–10 years after. *Tuberculosis (Edinb)*, **91**, 1–7.

Lewis, M. (2011) A tale of two repressors. *Journal of Molecular Biology*, **409**, 14–27.

Livak, K.J. and Schmittgen, T.D. (2001) Analysis of relative gene expression data using real-time quantitative

PCR and the 2(-Delta Delta C(T)) method. *Methods*, **25**, 402–408.

Lowrie, D.B., Aber, V.R. and Jackett, P.S. (1979) Phagosome-Lysosome Fusion and Cyclic Adenosine 3′: 5′-Monophosphate in Macrophages Infected with *Mycobacterium microti*, *Mycobacterium bovis* BCG or *Mycobacterium lepraemurium*. *Microbiology*, **110**, 431–441.

Luo, H., Zeng, J., Huang, Q., Liu, M., Abdalla, A.E., Xie, L. *et al*. (2016) *Mycobacterium tuberculosis* Rv1265 promotes mycobacterial intracellular survival and alters cytokine profile of the infected macrophage. *Journal of Biomolecular Structure and Dynamics*, **34**, 585–599.

Majumdar, S.D., Vashist, A., Dhingra, S., Gupta, R., Singh, A., Challu, V.K. (2012) Appropriate DevR (DosR)-mediated signaling determines transcriptional response, hypoxic viability and virulence of *Mycobacterium tuberculosis*. *PLoS One*, **7**, e35847.

Malen, H., Pathak, S., Softeland, T., de Souza, G.A. and Wiker, H.G. (2010) Definition of novel cell envelope associated proteins in Triton X-114 extracts of *Mycobacterium tuberculosis* H37Rv. *BMC Microbiology*, **10**, 132.

Mao, C., Shukla, M., Larrouy-Maumus, G., Dix, F.L., Kelley, L.A., Sternberg, M.J. *et al*. (2013) Functional assignment of *Mycobacterium tuberculosis* proteome revealed by genome-scale fold-recognition. *Tuberculosis (Edinb)*, **93**, 40–46.

Marino-Ramirez, L., Minor, J.L., Reading, N. and Hu, J.C. (2004) Identification and mapping of self-assembling protein domains encoded by the *Escherichia coli* K-12 genome by use of repressor fusions. *Journal of Bacteriology*, **186**, 1311–1319.

Mazandu, G.K. and Mulder, N.J. (2012) Function prediction and analysis of mycobacterium tuberculosis hypothetical proteins. *International Journal of Molecular Sciences*, **13**, 7283–7302.

McDonough, K.A. and Kress, Y. (1995) Cytotoxicity for lung epithelial cells is a virulence-associated phenotype of *Mycobacterium tuberculosis*. *Infection and Immunity*, **63**, 4802–4811.

McDonough, K.A., Kress, Y. and Bloom, B.R. (1993) Pathogenesis of tuberculosis: interaction of *Mycobacterium tuberculosis* with macrophages. *Infection and Immunity*, **61**, 2763–2773.

Mehra, S., Foreman, T.W., Didier, P.J., Ahsan, M.H., Hudock, T.A., Kissee, R. *et al*. (2015) The DosR regulon modulates adaptive immunity and is essential for *Mycobacterium tuberculosis* persistence. *American Journal of Respiratory and Critical Care Medicine*, **191**, 1185–1196.

Menozzi, F.D., Reddy, V.M., Cayet, D., Raze, D., Debrie, A.S., Dehouck, M.P. *et al*. (2006) *Mycobacterium tuberculosis* heparin-binding haemagglutinin adhesin (HBHA) triggers receptor-mediated transcytosis without altering the integrity of tight junctions. *Microbes and Infection*, **8**, 1–9.

Menozzi, F.D., Rouse, J.H., Alavi, M., Laude-Sharp, M., Muller, J. *et al*. (1996) Identification of a heparin-binding hemagglutinin present in mycobacteria. *The Journal of Experimental Medicine*, **184**, 993–1001.

Mueller-Ortiz, S.L., Sepulveda, E., Olsen, M.R., Jagannath, C., Wanger, A.R. and Norris, S.J. (2002) Decreased infectivity despite unaltered C3 binding by a hbhA mutant of *Mycobacterium tuberculosis*. *Infection and Immunity*, **70**, 6751–6760.

Murray, H., Ferreira, H. and Errington, J. (2006) The bacterial chromosome segregation protein Spo0J spreads along DNA from parS nucleation sites. *Molecular Microbiology*, **61**, 1352–1361.

Nambi, S., Gupta, K., Bhattacharyya, M., Ramakrishnan, P., Ravikumar, V., Siddiqui, N. (2013) Cyclic AMP-dependent protein lysine acylation in mycobacteria regulates fatty acid and propionate metabolism. *Journal of Biological Chemistry*, **288**, 14114–14124.

Pai, M., Behr, M.A., Dowdy, D., Dheda, K., Divangahi, M., Boehme, C.C. *et al*. (2016) Tuberculosis. *Nature Reviews Disease Primers*, **2**, 16076.

Pelly, S., Bishai, W.R. and Lamichhane, G. (2012) A screen for non-coding RNA in *Mycobacterium tuberculosis* reveals a cAMP-responsive RNA that is expressed during infection. *Gene*, **500**, 85–92.

Pethe, K., Alonso, S., Biet, F., Delogu, G., Brennan, M.J., Locht, C. *et al*. (2001) The heparin-binding haemagglutinin of *M. tuberculosis* is required for extrapulmonary dissemination. *Nature*, **412**, 190–194.

Ramsugit, S., Pillay, B. and Pillay, M. (2016) Evaluation of the role of *Mycobacterium tuberculosis* pili (MTP) as an adhesin, invasin, and cytokine inducer of epithelial cells. *The Brazilian Journal of Infectious Diseases*, **20**, 160–165.

Ranganathan, S., Bai, G., Lyubetskaya, A., Knapp, G.S., Peterson, M.W., Gazdik, M. *et al*. (2016) Characterization of a cAMP responsive transcription factor, Cmr (Rv1675c), in TB complex mycobacteria reveals overlap with the DosR (DevR) dormancy regulon. *Nucleic Acids Research*, **44**, 134–151.

Rao, S.P., Alonso, S., Rand, L., Dick, T. and Pethe, K. (2008) The protonmotive force is required for maintaining ATP homeostasis and viability of hypoxic, nonreplicating *Mycobacterium tuberculosis*. *Proceedings of the National Academy of Sciences of the United States of America*, **105**, 11945–11950.

Reddy, V.M. and Hayworth, D.A. (2002) Interaction of *Mycobacterium tuberculosis* with human respiratory epithelial cells (HEp-2). *Tuberculosis (Edinb)*, **82**, 31–36.

Rickman, L., Scott, C., Hunt, D.M., Hutchinson, T., Menendez, M.C., Whalan, R. *et al*. (2005) A member of the cAMP receptor protein family of transcription regulators in *Mycobacterium tuberculosis* is required for virulence in mice and controls transcription of the rpfA gene coding for a resuscitation promoting factor. *Molecular Microbiology*, **56**, 1274–1286.

Sassetti, C.M., Boyd, D.H. and Rubin, E.J. (2003) Genes required for mycobacterial growth defined by high density mutagenesis. *Molecular Microbiology*, **48**, 77–84.

Sassetti, C.M. and Rubin, E.J. (2003) Genetic requirements for mycobacterial survival during infection. *Proceedings of the National Academy of Sciences of the United States of America*, **100**, 12989–12994.

Schlesinger, L.S. (1993) Macrophage phagocytosis of virulent but not attenuated strains of *Mycobacterium*

tuberculosis is mediated by mannose receptors in addition to complement receptors. *Journal of Immunology*, **150**, 2920–2930.
Schnappinger, D., Ehrt, S., Voskuil, M.I., Liu, Y., Mangan, J.A., Monahan, I.M. *et al*. (2003) Transcriptional Adaptation of *Mycobacterium tuberculosis* within Macrophages: Insights into the Phagosomal Environment. *Journal of Experimental Medicine*, **198**, 693–704.
Schorey, J.S., Carroll, M.C. and Brown, E.J. (1997) A macrophage invasion mechanism of pathogenic mycobacteria. *Science*, **277**, 1091–1093.
Schreiter, E.R. and Drennan, C.L. (2007) Ribbon-helix-helix transcription factors: variations on a theme. *Nature Reviews Microbiology*, **5**, 710–720.
Schuck, P. (2000) Size-distribution analysis of macromolecules by sedimentation velocity ultracentrifugation and lamm equation modeling. *Biophysical Journal*, **78**, 1606–1619.
Seshasayee, A.S., Sivaraman, K. and Luscombe, N.M. (2011) An overview of prokaryotic transcription factors: a summary of function and occurrence in bacterial genomes. *Subcellular Biochemistry*, **52**, 7–23.
Sharp, J.D., Singh, A.K., Park, S.T., Lyubetskaya, A., Peterson, M.W., Gomes, A.L. *et al*. (2016) Comprehensive definition of the SigH regulon of *Mycobacterium tuberculosis* reveals transcriptional control of diverse stress responses. *PLoS One*, **11**, e0152145.
Shi, L., Sohaskey, C.D., Kana, B.D., Dawes, S., North, R.J., Mizrahi, V. *et al*. (2005) Changes in energy metabolism of *Mycobacterium tuberculosis* in mouse lung and under in vitro conditions affecting aerobic respiration. *Proceedings of the National Academy of Sciences of the United States of America*, **102**, 15629–15634.
Shi, L., Sohaskey, C.D., Pheiffer, C., Datta, P., Parks, M., McFadden, J. *et al*. (2010) Carbon flux rerouting during *Mycobacterium tuberculosis* growth arrest. *Molecular Microbiology*, **78**, 1199–1215.
Smith, L.J., Bochkareva, A., Rolfe, M.D., Hunt, D.M., Kahramanoglou, C., Braun, Y. *et al*. (2017) Cmr is a redox-responsive regulator of DosR that contributes to *M. tuberculosis* virulence. *Nucleic Acids Research*, **45**(11), 6600–6612.
Tews, I., Findeisen, F., Sinning, I., Schultz, A., Schultz, J.E. and Linder, J.U. (2005) The structure of a pH-sensing mycobacterial adenylyl cyclase holoenzyme. *Science*, **308**, 1020–1023.
Tsai, M.C., Chakravarty, S., Zhu, G., Xu, J., Tanaka, K., Koch, C. *et al*. (2006) Characterization of the tuberculous granuloma in murine and human lungs: cellular composition and relative tissue oxygen tension. *Cellular Microbiology*, **8**, 218–232.
Vasudeva-Rao, H.M. and McDonough, K.A. (2008) Expression of the *Mycobacterium tuberculosis* acr-coregulated genes from the DevR (DosR) regulon is controlled by multiple levels of regulation. *Infection and Immunity*, **76**, 2478–2489.
Velasco-Velazquez, M.A., Barrera, D., Gonzalez-Arenas, A., Rosales, C. and Agramonte-Hevia, J. (2003) Macrophage-*Mycobacterium tuberculosis* interactions: role of complement receptor 3. *Microbial Pathogenesis*, **35**, 125–131.
Via, L.E., Lin, P.L., Ray, S.M., Carrillo, J., Allen, S.S., Eum, S.Y. *et al*. (2008) Tuberculous granulomas are hypoxic in guinea pigs, rabbits, and nonhuman primates. *Infection and Immunity*, **76**, 2333–2340.
Vidal Pessolani, M.C., de Melo Marques, M.A., Reddy, V.M., Locht, C. and Menozzi, F.D. (2003) Systemic dissemination in tuberculosis and leprosy: do mycobacterial adhesins play a role? *Microbes and Infection*, **5**, 677–684.
Voskuil, M.I., Visconti, K.C. and Schoolnik, G.K. (2004) *Mycobacterium tuberculosis* gene expression during adaptation to stationary phase and low-oxygen dormancy. *Tuberculosis (Edinb)*, **84**, 218–227.
Wang, L. and Brown, S.J. (2006) BindN: a web-based tool for efficient prediction of DNA and RNA binding sites in amino acid sequences. *Nucleic Acids Research*, **34**, W243–248.
Wayne, L.G. and Hayes, L.G. (1996) An in vitro model for sequential study of shiftdown of *Mycobacterium tuberculosis* through two stages of nonreplicating persistence. *Infection and Immunity*, **64**, 2062–2069.
Wayne, L.G. and Sohaskey, C.D. (2001) Nonreplicating persistence of mycobacterium tuberculosis. *Annual Review of Microbiology*, **55**, 139–163.
WHO. (2015) *Global Tuberculosis Report 2015*. World Health Organization, Geneva, Switzerland.
WHO. (2016) *Global Tuberculosis Report 2016*. World Health Organization, Geneva, Switzerland.
Wolfe, L.M., Veeraraghavan, U., Idicula-Thomas, S., Schürer, S., Wennerberg, K., Reynolds, R., Besra, G.S. and Dobos, K.M. (2013) A chemical proteomics approach to profiling the ATP-binding proteome of *Mycobacterium tuberculosis*. *Molecular & Cellular Proteomics*, **12**, 1644–1660.
Wu, F.L., Liu, Y., Jiang, H.W., Luan, Y.Z., Zhang, H.N., He, X. *et al*. (2017) The Ser/Thr protein kinase protein-protein interaction map of *M. tuberculosis*. Molecular & Cellular Proteomics, **16**, 1491–1506.
Zhang, A., Wassarman, K.M., Ortega, J., Steven, A.C. and Storz, G. (2002) The Sm-like Hfq protein increases OxyS RNA interaction with target mRNAs. *Molecular Cell*, **9**, 11–22.
Zhang, M., Chen, J.M., Sala, C., Rybniker, J., Dhar, N. and Cole, S.T. (2014) EspI regulates the ESX-1 secretion system in response to ATP levels in *Mycobacterium tuberculosis*. *Molecular Microbiology*, **93**, 1057–1065.
Zheng, X., Papavinasasundaram, K.G. and Av-Gay, Y. (2007) Novel substrates of *Mycobacterium tuberculosis* PknH Ser/Thr kinase. *Biochemical and Biophysical Research Communications*, **355**, 162–168.
Zimmerli, S., Edwards, S. and Ernst, J.D. (1996) Selective receptor blockade during phagocytosis does not alter the survival and growth of *Mycobacterium tuberculosis* in human macrophages. *American Journal of Respiratory Cell and Molecular Biology*, **15**, 760–770.

Supporting Information

Additional supporting information may be found online in the Supporting Information section at the end of the article.